

Université du Québec
INRS-Géoresources

**Géochimie isotopique des bio-gaz produits par un couvert organique déposé sur
les résidus miniers réactifs au site East Sullivan, Québec, Canada.**

Par
Douglas Pankewich
(B.Sc. Géologie)

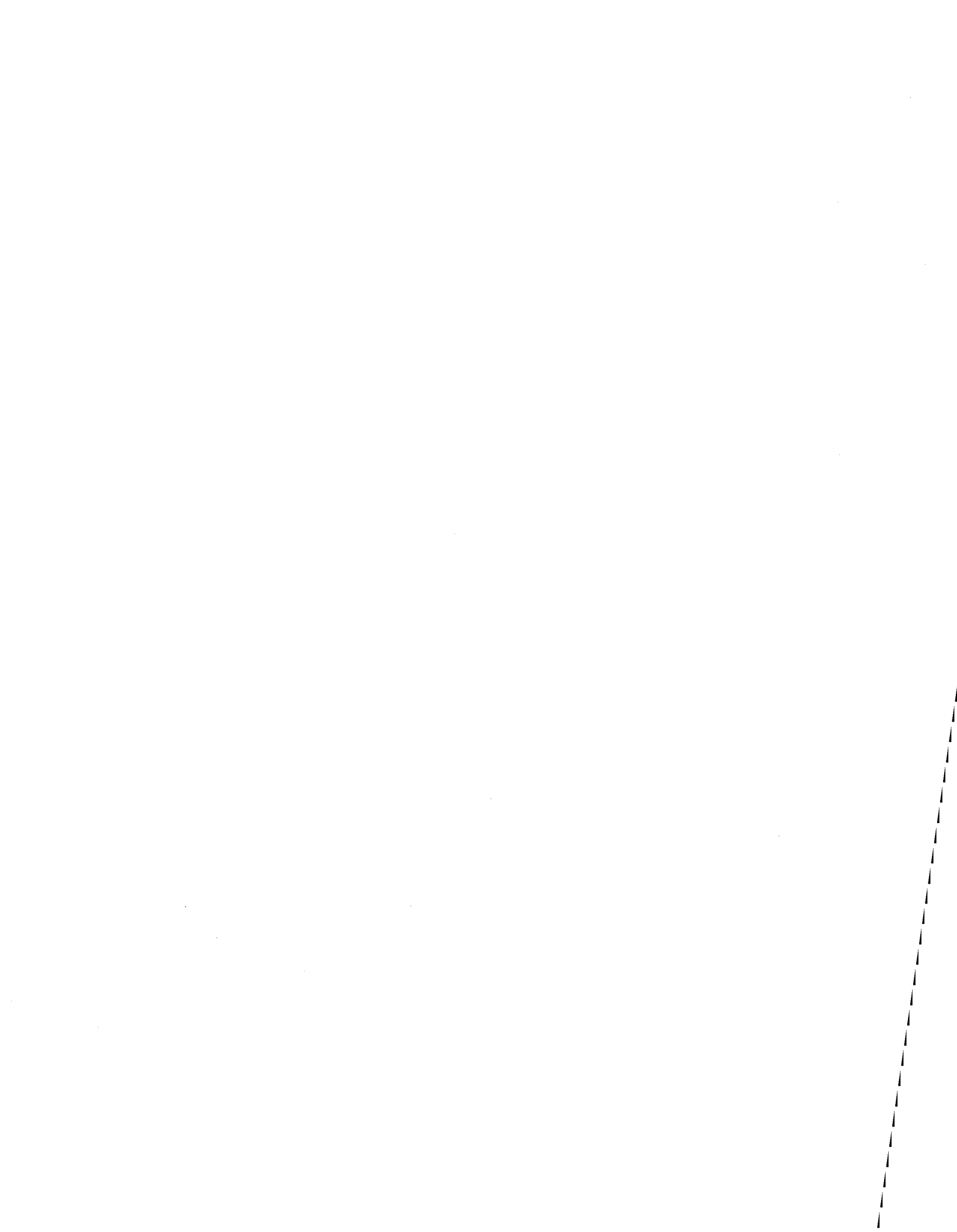
Mémoire présenté
pour l'obtention
du grade de Maître ès sciences (M.Sc.)

Jury d'évaluation

Examineur externe	Danielle Fortin Département des sciences de la terre Université d'Ottawa
Examineur interne	Yvon Héroux Centre géoscientifique de Québec Université du Québec
Codirectrice de recherche	Martine Savard Centre géoscientifique de Québec Commission géologique du Canada
Directeur de recherche	Normand Tassé Centre géoscientifique de Québec Université du Québec

Juillet, 1999

© droits réservés de Douglas Pankewich, 1999

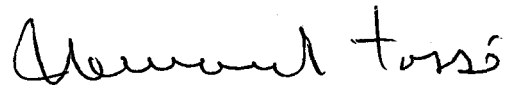


RÉSUMÉ • ABSTRACT

The isotopic signature of carbon from methane and carbon dioxide released by a reactive organic barrier overlaying the East Sullivan Mine tailings in Abitibi, Québec, was investigated to help evaluate its long-term efficiency. Concentration ratios between methane and carbon dioxide indicated that the activity associated with methanogenesis increased with the age of the organic materials. A comparison of the $\delta^{13}\text{C}$ values of coexisting methane and carbon dioxide indicated that fermentation as opposed to carbon dioxide reduction was the dominant production pathway for methane. This was true regardless of the age of the organic residues. That stability in biodegradation processes suggests that the long-term viability of the organic cover at East Sullivan may not be threatened by a decreasing efficiency, at least for the next decade.



Douglas Pankewich



Normand Tassé

Les résidus miniers du site East Sullivan (Abitibi, Québec) sont recouverts d'une barrière réactive de résidus ligneux. La composition isotopique du carbone des biogaz générés (méthane, bioxyde de carbone) a été déterminée, dans une perspective d'évaluation d'efficacité à long terme de cette couverture. Les rapports de concentration indiquent que la méthanogenèse est d'autant plus active que les résidus sont vieux. Les compositions isotopiques suggèrent par ailleurs que le méthane résulte principalement de processus de fermentation plutôt que d'une réduction de bioxyde de carbone, et ce dans tous les cas, sans égard à l'âge des résidus organiques. Compte tenu que les processus de réduction n'apparaissent qu'après épuisement de substrats facilement métabolisables, l'omniprésence des évidences de fermentation, y compris dans les résidus les plus vieux, suggère que la couverture ligneuse restera suffisamment réactive au moins pour la prochaine décennie.

ACKNOWLEDGEMENTS

I would like to express my sincere gratitude to my research directors Dr. Normand Tassé and Dr. Martine Savard for their help, guidance and interest. Their contributions to the successful completion of this project were enormous and I sincerely appreciate all of their efforts. I would also like to thank Mr. Marc Luzincourt for his advise and expertise concerning isotopic analysis and Dr. Karyne Rogers for introducing me to GC-C-IRMS analysis. Dr. Barbara Sherwood Lollar, Mr. Neil Arner and Mr. Edward Hornibrook are thanked for the information which they supplied to me with respect to proper sampling, handling and analytical techniques and Mr. Thomas Sommerville is thanked for his expertise with Autocad.

RÉSUMÉ EXTENSIF

Introduction

Les problèmes associés au drainage minier acide (DMA) ont été décrits aussi tôt qu'en 1698. Ceux-ci sont liés à l'oxydation des minéraux sulfureux par l'oxygène atmosphérique, dans des réactions chimiques catalysées par des bactéries. L'acide sulfurique et les métaux lourds ainsi mobilisés sont par la suite dispersés dans l'environnement. Quatre-vingt treize millions de tonnes de résidus miniers réactifs, au Québec, et plus d'un demi-milliard de tonnes, au Canada, peuvent générer du DMA. Des mesures correctives et préventives s'imposent en particulier dans des régions minières comme l'Abitibi, au Québec.

Les problèmes de DMA peuvent être résolus par prévention ou par traitement des effluents acides. Le traitement à long terme n'est pas souhaitable, à cause des durées très longues d'altération impliquées, de l'ordre de plusieurs décennies, voire siècles. Les technologies mises de l'avant ou en développement misent donc plutôt sur la prévention. Elles ont pour objectif commun d'empêcher l'oxygène de l'air d'entrer en contact avec les minéraux sulfureux, soit par des barrières sèches (membrane, couverture multicouche), soit par des barrières humides (ennoiment). Une alternative est la barrière réactive, dans laquelle un substrat organique consomme l'oxygène plutôt que d'empêcher sa diffusion.

Cette dernière technologie est utilisée à échelle réelle au site East Sullivan, dans le nord-ouest québécois, avec des résidus ligneux produits par l'industrie forestière locale. Le couvert est présentement efficace, l'oxygène étant complètement consommé à moins de 0,5-0,7 m d'enfouissement. Cependant, l'efficacité à long terme n'est pas assurée. Une barrière réactive implique l'épuisement éventuel de réactifs, et il est nécessaire de s'assurer que ce type de couverture puisse durer au moins plusieurs dizaines d'années.

Afin d'évaluer l'espérance de vie d'un tel couvert organique, il est nécessaire d'identifier et comprendre les mécanismes de dégradation des matériaux ligneux. Dans cette optique, nous avons entrepris l'étude de la composition isotopique du carbone des bio-gaz échantillonnés dans les pores de la couverture ligneuse du site East Sullivan. Cent quarante-sept échantillons de gaz biogènes ont ainsi été prélevés à intervalles successifs de 0,1 m à 13 stations différentes du site, en octobre 1996. Les analyses isotopiques du carbone ont été réalisées en CG-C-SMI (chromatographie gazeuse-combustion-spectrométrie de masse isotopique) au Delta-Lab de la Commission géologique du Canada à Sainte-Foy.

Le site East Sullivan et ses résidus forestiers

La mine East Sullivan, localisée à environ 7 km au sud-est de la ville de Val d'Or, en Abitibi, a été active de 1949 et 1966. Pendant cette période, 15 millions de tonnes de résidus pyriteux avec une concentration moyenne de 3,6 % S ont été générés. Les résidus remplissent sur 2 à 14 m d'épaisseur un parc de 136 hectares surplombant une plaine de marécages et boisés. Le parc est ceinturé de digues captant les effluents acides. Le potentiel générateur d'acidité des résidus est de 108,9 kilogrammes de carbonate de calcium par tonne, tandis que le potentiel neutralisant est de seulement 4,1 kilogramme par tonne. Avec une capacité vingt sept fois plus grande de générer de l'acide que d'en neutraliser, le site East Sullivan était donc une source importante de DMA appelée à persister pendant encore au moins plusieurs décennies.

La mise en place du recouvrement ligneux s'est amorcé en 1984 dans le secteur nord du parc, avec des résidus mixtes conifères-feuillus produits par une usine de panneaux particules. Depuis 1992, une usine de sciage répand également des résidus de conifères dans le secteur sud. Le recouvrement fait de 2 à 6 m d'épaisseur. Des boues de l'usine

d'épuration de Val d'Or sont déposées en surface pour compenser la déficience en azote des résidus ligneux et permettre la croissance de végétation.

Méthodologie

Les résidus forestiers recouvrant le parc ont été subdivisés et échantillonnés en fonction de leur composition et de leur âge (mixtes: 1984-90, 1990-94, 1994-96; résineux: 1992-94, 1994-96). Les échantillons gazeux étaient prélevés dans des seringues à l'aide d'un tube à pointe perforée enfoncé progressivement dans les résidus. Une succession systématique de purges et d'échantillonnage permettait d'obtenir des gaz représentatifs du milieu poreux souterrain à intervalles de 0,1 m. Les gaz recueillis étaient ensuite transférés intégralement dans des bouteilles de verre fermées par des septum à membrane de téflon, jusqu'à ce qu'ils soient analysés.

Les analyses ont fait appel à la technologie CG-C-SMI. Dans ce système, des gaz mélangés (e.g. CO₂ et CH₄) sont ajoutés à un gaz porteur d'hélium. Ils sont séparés par chromatographie en phase gazeuse (CG), puis subissent tour à tour une oxydation en CO₂ par combustion (C), s'ils ne sont pas déjà sous cette forme. Ces gaz sont ensuite dirigés en continu vers un spectromètre de masse à source gazeuse pour détermination des rapports isotopiques du carbone (SMI). Concrètement, le chromatographe Hewlett Packard 5890 Series II, équipé d'une colonne capillaire Chromopack de type PoraPlot-Q, était utilisé à température ambiante (25-28°C isotherme) à pression d'entrée de 12 psi, débit de 20 ml/min et température de l'injecteur de 250°C. Sous ces conditions, les temps de rétention du méthane et du bioxyde de carbone étaient de 215 et 250 secondes, respectivement. La combustion se faisait à 900°C dans une fournaise à tube de quartz rempli de CuO. L'eau et autres gaz non désirables étaient condensés dans un bain cryogénique avant analyse dans le spectromètre de masse, un Fisons Isotech Prism III à quadruple collecteurs. Trois de ces collecteurs, positionnés aux masses 44, 45 et 46,

permettaient de déterminer le rapport isotopique du carbone. Un gaz de référence, injecté deux fois avant et deux fois après chacun des échantillons analysés, permettait un dosage en fonction d'un standard international (NBS-19, PDB). Divers tests ont été réalisés pour s'assurer de la combustion quantitative du méthane lors des analyses, ainsi que de la bonne représentativité des échantillons conservés avec la méthode préconisée.

Résultats

Le méthane et le bioxyde de carbone constituent l'essentiel des gaz interstitiels de la couverture ligneuse à East Sullivan, en plus de l'azote et de l'oxygène. À défaut de concentrations absolues, nos résultats nous permettent tout de même de connaître les abondances relatives du méthane et du bioxyde de carbone, car les analyses portaient sur des gaz coexistants dans le même aliquot analysé. Il suffit de faire le rapport des aires sous les pics de méthane et de bioxyde de carbone mesurés aux collecteurs du spectromètre de masse et de multiplier le résultat par 100 pour obtenir un "rapport de concentration". Ce rapport variait de 0 (pas de méthane) à 625 (6,25 fois plus de méthane que de bioxyde de carbone) dans les échantillons analysés.

Le rapport de concentration varie en fonction de l'âge des résidus forestiers. Ainsi, le méthane est relativement plus abondant dans les résidus antérieurs à 1990 (rapport moyen de 240, pour l'ensemble des échantillons prélevés à 0,5 m) que dans ceux de 1992 à 1996 (rapport moyen inférieur ou égal à 21). Le rapport de concentration varie aussi en fonction de la localisation de la station d'échantillonnage. Ainsi, les stations situées en bordure de couverture ou de zone plus perméable, dans les résidus anciens, montrent des rapports systématiquement inférieurs à la moyenne du groupe (139 et moins). Enfin, le rapport de concentration augmente avec la profondeur, par un facteur pouvant facilement atteindre un ordre de grandeur.

Le domaine de variation des valeurs de $\delta^{13}\text{C}$ est beaucoup plus restreint pour le bioxyde de carbone (-24‰ à -10‰) que pour le méthane (-75‰ à -20‰). Les profils de $\delta^{13}\text{C}_{\text{CO}_2}$ sont généralement réguliers, avec des valeurs augmentant vers le bas à raison de 0 à 5‰/m, jusqu'à 17,5‰/m dans la partie supérieure des profils. Les moyennes des résultats par station, à 0,7 m et plus (gradients moins prononcés), semblent plus élevées dans les vieux résidus que dans les résidus récents (-16‰ à -10‰ vs -19‰ à -16‰). Toutefois, il s'agit d'une tendance plutôt qu'une systématique. Les profils de $\delta^{13}\text{C}_{\text{CH}_4}$ sont également réguliers, mais avec des valeurs diminuant vers le bas dans tous les cas sauf un, dans la partie supérieure des profils (jusqu'à 50‰/m), et presque invariant à plus grande profondeur. Les moyennes par station, à 0,7 m et plus, sont relativement regroupées et vont de -53‰ à -45‰ dans 7 cas sur 9. Les deux autres se situent à -31‰ et -29‰. Aucune particularité ne peut être associée à ces deux valeurs élevées.

Les résultats montrent que le méthane est sujet à un plus grand fractionnement isotopique que le bioxyde de carbone, et que ce fractionnement est surtout présent dans la partie supérieure des profils. Pour les besoins de la discussion, le couvert organique est subdivisé en deux unités distinctes. La première (Zone A) est située entre la surface et une profondeur de 0,7 à 0,8 m. La deuxième (Zone B) se trouve entre la zone A et la surface de la nappe phréatique (ou la base du couvert organique). La limite exacte entre les deux zones peut varier, dépendant des différences locales de perméabilité des résidus forestiers, de réactivité de la matière organique et de température.

Discussion

L'oxydation du carbone par l'oxygène atmosphérique correspond au remplacement stoechiométrique de O_2 par CO_2 dans la partie supérieure des profils. En milieu anaérobie, le bioxyde de carbone peut également être produit par des réactions utilisant d'autres

oxidants que l'oxygène (*e.g.* oxyhydroxydes de fer ou de manganèse, nitrates, sulfates). Le méthane est une étape terminale de dégradation de matière organique.

Le méthane biogène peut être produit par deux types de réaction, *i.e.* fermentation et réduction du bioxyde de carbone. La fermentation (terme collectif désignant l'hydrogénation des groupes méthyls d'acétate, méthanol, méthyle-amines, etc.) génère à la fois du méthane et du bioxyde de carbone, ce dernier s'ajoutant à celui produit par oxydation. Ce méthane est appauvri en ^{13}C et en deutérium (D) ($\delta^{13}\text{C} = -65\text{‰}$ à -50‰ , $\delta\text{D} = -400\text{‰}$ à -250‰). La réduction du bioxyde de carbone produit un méthane encore plus allégé en ^{13}C , mais moins appauvri en D ($\delta^{13}\text{C} = -110\text{‰}$ à -60‰ , $\delta\text{D} = -250\text{‰}$ à -170‰). Les deux mécanismes peuvent coexister, mais la prédominance de l'un sur l'autre dépend essentiellement des qualités du substrat organique et de la température. À température égale, la disponibilité de composés réactifs favorise la fermentation. L'épuisement du réservoir de matière facilement métabolisable permet l'apparition des mécanismes de réduction.

Les propriétés physiques de la couverture ligneuse du parc East Sullivan sont plutôt uniformes, de telle sorte que c'est essentiellement l'âge et la nature des substrats organiques qui contrôleront le type de méthanogenèse. Comme la réduction de CO_2 remplace la fermentation avec l'épuisement de matière organique facilement réactive, déterminer l'importance relative des deux filières revient à déterminer à quel point la couverture ligneuse contient des substrats métabolisables propre à assurer la méthanogenèse et la consommation d'oxygène dans le futur.

L'identification d'une ou l'autre filière productrice de méthane peut être réalisée en comparant les résultats de $\delta^{13}\text{C}$ de méthane et de bioxyde de carbone coexistants à des champs spécifiques définis par la compilation de données isotopiques d'environnements méthanogènes connus. Les résultats d'East Sullivan sont majoritairement assimilables au

processus de fermentation. Les échantillons faisant exception sont localisés à faible profondeur (zone A) ou en bordure du couvert organique. Dans ces cas, la signature isotopique est oblitérée par l'oxydation du méthane par l'oxygène atmosphérique. La distorsion touche surtout le $\delta^{13}\text{C}$ du méthane quand le rapport de concentration indique une proportion élevée de bioxyde de carbone. À l'opposé, c'est surtout le $\delta^{13}\text{C}$ du bioxyde de carbone qui est affecté quand c'est la proportion de méthane qui est élevée. Une seule station, la plus jeune, montre ce qui semble être véritablement une réduction de carbonates. L'identification d'un processus caractéristique de dégradation d'un milieu organique réfractaire dans des résidus qui devraient être les plus réactifs de par leur âge suggère qu'une période de dégradation préalable est présente, et que la fermentation s'exerce sur des composés biodégradés plutôt que sur les résidus ligneux eux-mêmes.

Compte tenu de la prédominance de la filière de fermentation, on peut affirmer que la source de la matière organique disponible pour la biodégradation dans le système biogène du couvert organique est encore immature.

Sommaire et conclusion

La couverture de résidus ligneux montre deux zones distinctes. La première (zone A), peu profonde, englobe la zone de diffusion de l'oxygène atmosphérique et persiste jusqu'à sa consommation totale par l'oxydation du carbone. La seconde (zone B), plus profonde (jusqu'à la nappe phréatique), est caractérisée par des conditions anaérobies où il peut y avoir méthanogenèse. La profondeur de l'interface entre les deux zones (0,5-0,7 m) dépend de la porosité et de la perméabilité des résidus forestiers, de leur réactivité et de leur température. La zone A montre des gradients de CH_4/CO_2 , de $\delta^{13}\text{C}_{\text{CH}_4}$ et de $\delta^{13}\text{C}_{\text{CO}_2}$ élevés, alors que les gradients sont nuls ou faibles dans la zone B.

Les concentrations de CH_4 par rapport à CO_2 augmentent vers le bas, *i.e.* vers la zone B, où le méthane est généré. Le méthane est communément plus abondant dans les résidus anciens (≤ 1990) que dans les résidus plus récents (≥ 1992), ce qui suggère qu'un certain degré de décomposition, et non seulement des conditions anaérobies, sont requises pour la production de quantités significatives de méthane.

La composition isotopique du carbone du méthane varie beaucoup plus que celle du carbone du bioxyde de carbone. Les gradients de $\delta^{13}\text{C}_{\text{CH}_4}$, extrêmes dans la zone A (décroissants, de -15‰ à -50‰/m), sont plus stables en zone B (0‰ à -8‰/m). Les gradients de $\delta^{13}\text{C}_{\text{CO}_2}$ sont moindres et à l'inverse (croissants, de 0‰ à 18‰/m). Les diagrammes de $\delta^{13}\text{C}_{\text{CH}_4}$ vs $\delta^{13}\text{C}_{\text{CO}_2}$ montrent que le méthane est produit par fermentation. Cette signature est oblitérée par l'oxydation du méthane dans la zone A, qui déplace de façon perceptible $\delta^{13}\text{C}_{\text{CH}_4}$ vers des valeurs plus grandes, lorsque le milieu ne contient pas trop de méthane, et pousse $\delta^{13}\text{C}_{\text{CO}_2}$ vers des valeurs plus faibles, lorsque le milieu ne contient pas trop de bioxyde de carbone. Un gradient de $7,5\text{‰/m}$ est observé pour $\delta^{13}\text{C}_{\text{CO}_2}$ dans une station réalisée dans des résidus miniers, à l'écart de la couverture organique, et sans méthane. Les gradients sont donc attribuables à un fractionnement impliquant des phases dissoutes ou solides qui ne sont pas nécessairement organiques.

Les valeurs moyennes de $\delta^{13}\text{C}_{\text{CH}_4}$ et de $\delta^{13}\text{C}_{\text{CO}_2}$ de la zone B, où ces valeurs sont les plus stables, ne peuvent être mises en corrélation avec le type ou l'âge des résidus. Seule une tendance à observer des valeurs de $\delta^{13}\text{C}_{\text{CO}_2}$ quelque peu plus élevées dans les résidus anciens est notée. Si l'on excepte deux stations où le méthane a subi une oxydation importante, les valeurs de $\delta^{13}\text{C}$, tant pour le méthane que pour le bioxyde de carbone, varient à l'intérieur de 10‰ .

Nos résultats ne permettent pas de définir une période précise pour laquelle les résidus forestiers permettront de bloquer efficacement l'accès de l'oxygène aux sulfures. Toutefois, le fait que le méthane soit produit essentiellement par fermentation dans l'ensemble de la couverture suggère que le réservoir de matière organique est suffisamment réactif pour que la couverture soit fonctionnelle encore plusieurs années.

TABLE OF CONTENTS

RÉSUMÉ • ABSTRACT	i
ACKNOWLEDGEMENTS	iii
RÉSUMÉ EXTENSIF	v
LIST OF FIGURES	xvii
LIST OF TABLES	xix
INTRODUCTION.....	1
CHAPTER 1	
THE EAST SULLIVAN MINE.....	5
1.1 General statement	5
1.2 Previous investigations.....	9
1.3 Research goals.....	10
CHAPTER 2	
METHODOLOGY	11
2.1 Field sampling and sample preservation	11
2.2 Isotopic analyses	14
2.2.1 Gas chromatography	15
2.2.2 Combustion and injection concentrations.....	15
2.2.3 Mass spectrometry	16
2.2.4 Precision and reliability of results	20
CHAPTER 3	
RESULTS	21
3.1 Methane/carbon dioxide concentration ratios.....	21
3.2 Carbon isotope ratios of methane and carbon dioxide	25
CHAPTER 4	
DISCUSSION	33
4.1 Biogenic gases and methanogenesis	33
4.2 Methanogenic production pathways.....	34
4.3 The dominating methane production pathway at East Sullivan	37
4.4 Proposed model for the carbon cycle in the organic cover	43
4.5 Special case: Station C12	47
CONCLUSION AND RECOMMENDATIONS.....	49
REFERENCES.....	51
APPENDIX A.....	55
APPENDIX B	67

LIST OF FIGURES

Figure 1.	Map of the study site, including the locations of all sampling stations	8
Figure 2.	Illustration of the sampling system employed during this study	12
Figure 3.	The GC-C-IRMS System	14
Figure 4.	Typical chromatogram obtained in GC-C-IRMS analyses	18
Figure 5.	Depth profiles of CH ₄ /CO ₂ concentration ratios in pore gases.....	22
Figure 6.	Depth profiles of isotopic results for carbon dioxide.....	26
Figure 7.	Depth profiles of isotopic results for methane.....	27
Figure 8.	Distribution of average $\delta^{13}\text{C}_{\text{CO}_2}$ and $\delta^{13}\text{C}_{\text{CH}_4}$ and relation with age and type of wood wastes.....	29
Figure 9.	Relative degree of importance of each of the methanogenic production pathways.....	35
Figure 10.	Cross-plot of $\delta^{13}\text{C}$ for methane-carbon dioxide pairs in the pore gases of the wood waste cover, all samples	39
Figure 11.	Cross-plot of $\delta^{13}\text{C}$ for methane-carbon dioxide pairs in the pore gases of the wood waste cover, excluding shallow and/or near-margin samples.....	40
Figure 12.	Cross-plot of $\delta^{13}\text{C}$ of coexisting CO ₂ and CH ₄ in the pore gases of the wood waste cover.....	41
Figure 13.	Simplified model of the carbon cycle in the organic cover.....	46
Photographs 1-4.	Site Photographs.....	Appendix A
Figures B-1 to B-13.	Depth profiles of isotopic results for carbon dioxide and methane from individual stations.....	Appendix B
Figures B-14 to B-19.	Cross-plot of the carbon isotope ratios of methane and carbon dioxide of Stations C1, C4, C6, C7, C12, C13, C14, 0-8 and M11.....	Appendix B
Figures B-14 to B-19.	Cross-plot of the carbon isotope ratios of methane and carbon dioxide of Stations C1, C4, C6, C7, C12, C13	Appendix B

LIST OF TABLES

Table 1.	General characteristics of the organic cover at East Sullivan.....	7
Table 2.	Average values of CH ₄ /CO ₂ concentration ratios at 0.5 m according to age and type of wood wastes	23
Table 3.	Summary of $\delta^{13}\text{C}_{\text{CO}_2}$ and $\delta^{13}\text{C}_{\text{CH}_4}$ results as average values and trends, for each station sampled.....	28
Table 4.	General properties of samples plotting outside the fermentation and CO ₂ reduction fields.....	42
Table A-1	Outline of procedures used to obtain the best possible separation of ion-current peaks	Appendix A
Tables A-2 to A-9	Laboratory tests and analytical verifications.....	Appendix A
Tables B-1 to B-14	Isotopic results from individual stations.....	Appendix B

INTRODUCTION

Acidity problems associated with the alteration of sulfide rich mine tailings have been documented since at least 1698 (Paine, 1987). These problems, commonly referred to as Acid Mine Drainage (AMD), are intrinsically related to the oxidation of sulfide minerals through chemical and biological reactions with oxygen, water and bacteria. The end products of these reactions include sulfuric acid, which mobilizes heavy metals, with consequent contamination of neighbouring ecosystems. It is estimated that, in the province of Québec alone, over ninety three million tons of sulfide rich mine tailings have an acidic potential. In all of Canada, that number increases to well over half a billion tons (Environment Canada, 1991). The potential problems associated with AMD are therefore enormous, and preventative measures are needed in mining districts such as the region of Abitibi, in northwestern Québec.

As a result of public pressure, increased government regulation and recent environmental "commitment" on the part of the mining industry, efforts are being made to decrease the production of AMD. In order to achieve a lasting solution to the problems associated with AMD, one is presented with two fundamental choices. The first choice is to act in a preventative manner and address the production mechanism associated with AMD while the second is to treat the resulting effluent waters. Unfortunately, due the great quantities of effluents involved and the extended period of time necessary for adequate treatment, it is often neither feasible nor economically viable to treat acidic effluent water at a mining site, at least following closure of the mine. As a result, much research has focused on developing new preventative technologies, the most promising aiming to cut off the oxygen supply to the reactive tailings.

One potential solution to the problems associated with AMD is the implementation of an impermeable cover which includes either a synthetic layer or a multi-layer soil cover (Blowes *et al.*, 1994). Unfortunately, these covers are often expensive and are susceptible to cracking and leaks once installed (Collin, 1987 in Blowes *et al.*, 1994).

A second possible solution to AMD problems is the use of an aqueous cover over reactive mine tailings. Oxygen has a slow diffusion rate within water and the availability of this reactant is therefore greatly decreased when compared to direct contact between the tailings and the atmosphere. As a result, the production of AMD is greatly reduced (Blowes *et al.*, 1994). However, several disadvantages are related to this type of solution, especially if both the tailings and water need to be confined by dams. Aqueous covers are often unattractive and expensive solutions due to the fact that the increased volume of water increases the risk of dam failure, that an increased hydraulic gradient may lead to an increased flow of water into the environment and that the pools require constant monitoring, must remain leak free and be resistant to degradation over a long period of time (Blowes *et al.*, 1994). Finally, another solution, which is being tested for the first time on a large scale at the East Sullivan mine tailings compound, is the use of a chemical rather than a physical barrier to oxygen. Forest residues have been placed over reactive mine tailings in order to consume atmospheric oxygen before it reaches reactive sulfide. The organic barrier concept was first proposed in the mid 1980's by Reardon and Poscente (1984) and Reardon and Moddle (1985). More recently, Tassé *et al.* (1997) proposed that such an organic cover could be incorporated into a semi-passive system for the treatment of acid-prone waters generated prior to cover placement.

In its early years the East Sullivan organic cover was composed of aspen, woodchips, resinous bark and trunks, and presswood fragments produced by the local lumber industry (Université de Sherbrooke, 1988 in Tassé *et al.*, 1994). However, since 1992 the supply of wood wastes has diversified to include mostly coniferous forest products, namely bark strips and chips (Tassé *et al.*, 1997). Tassé *et al.* (1994) demonstrated that this type of organic cover is efficient in acting as an oxygen barrier. As these materials biodegrade through a series of bacteriologically mediated reactions, they consume available oxygen and create carbon dioxide and methane. Available concentrations of oxygen therefore decline rapidly from the surface of the wood wastes.

In fact, depending on the location on the organic cover, these concentrations are completely exhausted at depths of 50 cm to 70 cm from the surface.

Some concerns regarding the long-term efficiency of such a reactive cover have been raised. In 1985, Reardon and Poscente investigated the loss of carbon as a result of oxidative degradation in wood piles constructed of materials similar to those found at East Sullivan. They estimated that the loss of carbon, mainly in the form of carbon dioxide, was equal to 13 cm/year. At East Sullivan, bio-mass removal rates calculated in a similar fashion were however lower, ranging from 0.5 to 5.8 cm/year (Tassé and Germain, 1996). These figures indicate that the wood wastes may, in the future, become sterile and unable to react with atmospheric oxygen, unless the reservoir of reactive carbon is replenished. There is thus a possibility that the production of AMD may resume.

The long-term viability and behaviour of such organic covers is one of the many unknown variables that needs to be clarified before they may be used as a systematic solution to AMD problems (Tassé *et al.*, 1997). As part of a commitment to understanding these unknown variables, a study of the carbon stable isotope composition of methane and carbon dioxide was undertaken. This study was completed in order to identify and understand the production mechanisms of the biogenic gases released by the organic cover at East Sullivan. In October of 1996, 147 pore gas samples were extracted from the organic cover at 13 different sampling stations. The extractions were completed at intervals of 10 cm. Each of the sampling stations was located in an area where the age and maturity of the organic wastes was different. Stable isotope analyses were subsequently completed using a Gas Chromatograph-Combustion-Isotope Ratio Mass Spectrometer (GC-C-IRMS) analytical system.

CHAPTER 1

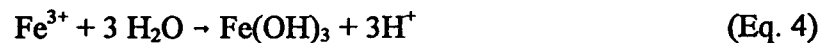
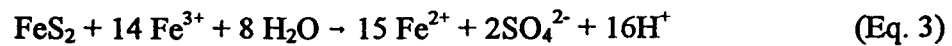
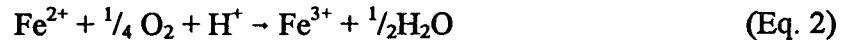
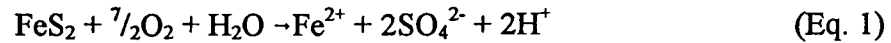
THE EAST SULLIVAN MINE

1.1 GENERAL STATEMENT

Since being labelled as one of the twenty eight most environmentally damaging sites in Québec, the East Sullivan mine in the region of Abitibi has become the focus of many investigations concerning its AMD problems. The mine site is located approximately 7 km south-east of Val d'Or and is accessible using a gravel service road south of Highway 117. The mine tailings impoundment is surrounded by lowlands (spruce trees and swamp) and is bordered by the Bourlamaque River to the east. Retention dikes have been constructed around the impoundment to collect effluent waters (Photos 1 - 4, Appendix A).

The East Sullivan mine was active from 1949 to 1966. During this time, 15 million tons of pyritic mine tailings with an average sulfur concentration of 3.6% were deposited at the site. They cover an area of approximately 1.36 km² (136 hectares) and range in thickness from 2-14 metres. The acid generating potential of the unaltered tailings is 108.9 kg of calcium carbonate per ton, whereas their acid neutralizing potential is 4.1 kg/ton (Tassé *et al.*, 1997). The tailings are therefore capable of producing approximately 27 times as much acidity as they are capable of neutralizing. The total acid generating potential, assuming non-oxidation of sulfide minerals in the saturated zone and 100% use of the neutralizing potential, was estimated by Tassé *et al.* (1997) to be 400 439 tons of calcium carbonate. It is therefore obvious that, without intervention, this impoundment would be a source of AMD for many decades.

As described by Tassé *et al.* (1997), the AMD problems experienced at East Sullivan are directly related to the presence of sulfide rich tailings that are openly exposed to atmospheric oxygen and water. The oxidation of pyrite either by oxygen (Equation 1) or by ferric iron (Equation 3) produces sulfate ions, ferrous iron and acid. The ferrous iron is then transformed through oxidation to ferric iron by oxygen and a proton (Equation 2). The resulting ferric iron will then proceed to either oxidize more pyrite or be hydrolysed (Equation 4). Oxidation and hydrolysis (Equations 2 and 4) of iron carried by groundwater can take place outside the impoundment, meaning that AMD can continue until the acid-prone pore water is purged from the system. A more precise description of this process, including the hydrogeology and acidity transport mechanism is provided by Tassé and Germain (1996) and Tassé *et al.* (1997).



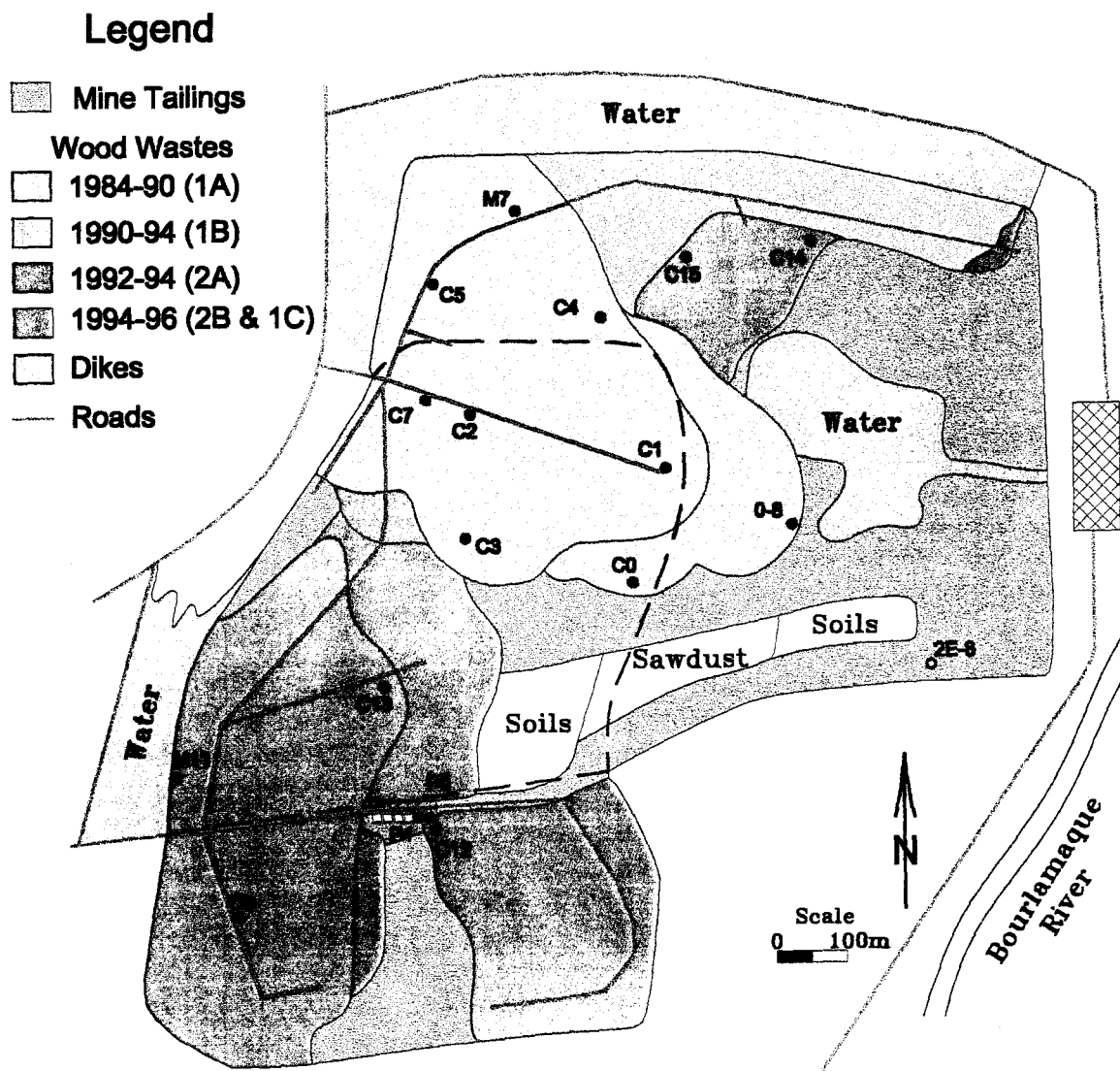
The organic cover installed on the East Sullivan site comprises wood wastes produced by local forest industry mills. Implementation of the organic cover began in the northwest area of the impoundment in 1984 with deposits from a particle board factory. Since 1992, a saw-mill plant has also been laying down wood wastes over the southwest sector of the site (Tassé *et al.*, 1997). For the purposes of this study, the wood wastes have been separated into two types according to their composition. Each type was subsequently subdivided into different groups, according to their age (Figure 1; Table 1). Type 1 materials cover the north and north-west sectors of the impoundment. It encompasses organic materials of a mixed coniferous and deciduous nature, mostly observed to be bark fragments, logs and presswood material. Group 1A comprises

deposits laid down between 1984 and 1990, piled in thickness ranging between 0.2 and 6 metres. Groups 1B and 1C feature similar but younger material (1B: 1990-1994; 1C: 1994-1996), levelled into a uniform 2 metre thickness. Type 2 wood wastes are located in the southwest sector of the impoundment and comprise mostly coniferous bark fragments, logs and sawdust, with an average thickness of 2 to 3 metres. Group 2A encompasses the older deposits, laid down between 1992 and 1994, whereas Group 2B features wood wastes laid down after 1994 (Tassé *et al.*, 1997). Sewage sludges have been applied to the wood wastes in some areas of the organic cover. This task was completed in order to compensate for a nitrogen deficiency within the wood residues and promote the growth of vegetation.

Table 1. General characteristics of the organic cover at East Sullivan.

Group (Sector)	Dominant Forest Residue Type	Deposition Date	Average Thickness (m)	Presence/Absence of Raw Sewage (per October 1996)
1A (northwest)	Mixed coniferous/deciduous	1984 - 1990	0.2 to 6.0	Area almost entirely overlain with raw sewage
1B (northwest)	Mixed coniferous/deciduous	1990 - 1994	1.5 to 2.0 m	Northwestern corner covered
1C (northwest)	Mixed coniferous/deciduous	1994 - 1996	2.0	Absent
2A (southwest)	Coniferous	1992 - 1994	2.0	A small patch near Station M11
2B (southwest)	Coniferous	1994 - 1996	2.0	Absent

Figure 1. Map of the study site, including the locations of all sampling stations.



East Sullivan Mine Tailings Park

1.2 PREVIOUS INVESTIGATIONS

Although the East Sullivan mine has been closed since 1966, no significant examination of its environmental impacts on the surrounding ecosystems was completed until the late 1980's (Planigram, 1987). Since that time, research and monitoring has been carried out by, amongst others, the Université de Sherbrooke, SNC-Lavalin, the Québec Ministry of Environment and Fauna, the Québec Ministry of Natural Resources and the INRS-Géoresources (Tassé and Germain., 1996, and references therein). Much of this work concerned the use of organic materials as a potential solution to the problems of Acid Mine Drainage (Université de Sherbrooke, 1988; Karam et Azzaria, 1990; CRIQ, 1991; Germain *et al.*, 1992; Paquet, 1992; Tassé *et al.*, 1994).

Research more specifically oriented towards the woodwaste cover at East Sullivan began in the early 1990's. Germain *et al.* (1992) and Tassé *et al.* (1994) demonstrated that the organic cover presently in place was indeed efficient as an oxygen barrier. Le Centre de recherche minérales (Québec Ministry of Natural Resources) also built and monitored several experimental parcels (Roche Ltée, 1994). That investigation confirmed that the organic cover is generally effective in its capacity as an oxygen barrier. Tassé and Germain (1996) completed a study of the groundwater quality and residual effluent waters released at the site. They recognized the positive overall benefits that the groundwater obtains from the wood wastes. Moreover, they indicated that the organic cover possesses other positive features: for instance, it causes a rise in the water table, which partially mimics an aqueous cover; and it is able to transmit enough alkalinity to the groundwater that it could be used in a semi-passive treatment system aimed at neutralizing acidity produced prior to full prevention of sulfide oxidation (Tassé *et al.*, 1997).

Concerns regarding the long-term efficiency of the organic cover were expressed by Tassé *et al.* (1994), after they observed relatively high biomass removal rates, comparable to those obtained by Reardon and Poscente (1984). These concerns were reiterated by Tassé and Germain (1996) after the acquisition of additional data on pore gases and dissolved organic carbon. It was recommended to obtain more data on the geochemical behaviour of the organic cover, in order to better evaluate its value as a long term option to the problems of AMD.

1.3 RESEARCH GOALS

This study is aimed at contributing to the fore-mentioned recommendation by Tassé and Germain (1996). The goal is to relate the effects of on-going biodegradational processes occurring within the woodwaste cover to the composition of the pore gases. For that purpose, vertical profiles were gathered at various locations over the East Sullivan impoundment by sampling interstitial gases at systematic depth intervals. Stable carbon isotopic compositions were determined for coexisting carbon dioxide and methane gases. This information permitted the determination of the production pathways by which these biogenic gases are being produced. Concentration ratios were used to evaluate the degree to which methane is present within the organic cover, relative to carbon dioxide, in order to identify the mechanisms that control their relative abundances.

CHAPTER 2 METHODOLOGY

2.1 FIELD SAMPLING AND SAMPLE PRESERVATION

Between the fifth and eleventh of October 1996, 147 gas aliquots were sampled from the East Sullivan site. Vertical profiles were sampled at 13 stations and spot sampling at 50 cm was completed at 5 additional stations. The distribution of the sampling stations according to type and age of wood wastes (Figure 1) is as follows:

Group 1A (mixed coniferous/deciduous, 1984-1990):

profiles: C1, C4, C7, M7, 0-8 spot samples: C0, C2, C3, C5

Group 1C (mixed coniferous/deciduous, 1994-1996):

profiles: C14, C15 spot samples: none

Group 2A (coniferous, 1992-1994):

profiles: C6, C13, M11, P4 spot sample: P5

Group 2B (coniferous, 1994-1996):

profiles: C12 spot samples: none

Tailings without a woodwaste cover:

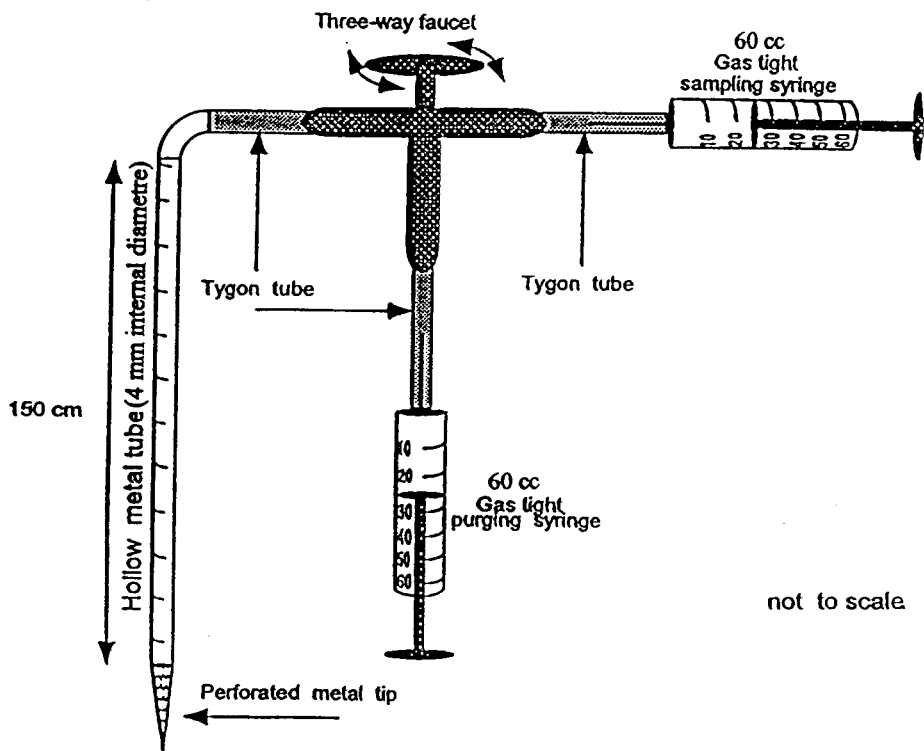
profile: 2E-8 spot samples: none

That sampling strategy allows comparison of pore gases from Type 1 and Type 2 wood wastes, without any overlying sewage, for the years 1990-92 (0-8 vs C6), 1994 (C15 vs C13), and 1996 (C14 vs C12). Effects of sewage incorporation can be evaluated on old and young Type 1 wood wastes (C1, C4 and M7, laid down approximately in 1989, 1989 and 1990, and overlain with sewage in 1990, 1992 and 1993). Some stations were also sampled for specific reasons: C7 features the oldest wood wastes known on the site (1984; date of sewage deposition unknown); P4 is from an experimental plot where pore gases composition was monitored from 1992 to 1994; self-combustion was observed in 1994 at M11, two year after deposition. Finally, Station 2E-8

allows comparison of biogenic CO₂ gas profiles with a CO₂ profile derived mainly from acid neutralization by carbonate minerals, in woodwaste-free tailings.

All samples were collected using the system illustrated in Figure 2. The apparatus consisted of a hollow metal tube (4 mm internal diameter, 1.5 m long) with a perforated tip attached to a three-way glass stopcock. The other two openings of the stopcock were connected to two 60 cc plastic gas tight syringes, one dedicated to the purge of the sampling line, the other to the sample itself.

Figure 2. Illustration of the sampling system employed during this study.



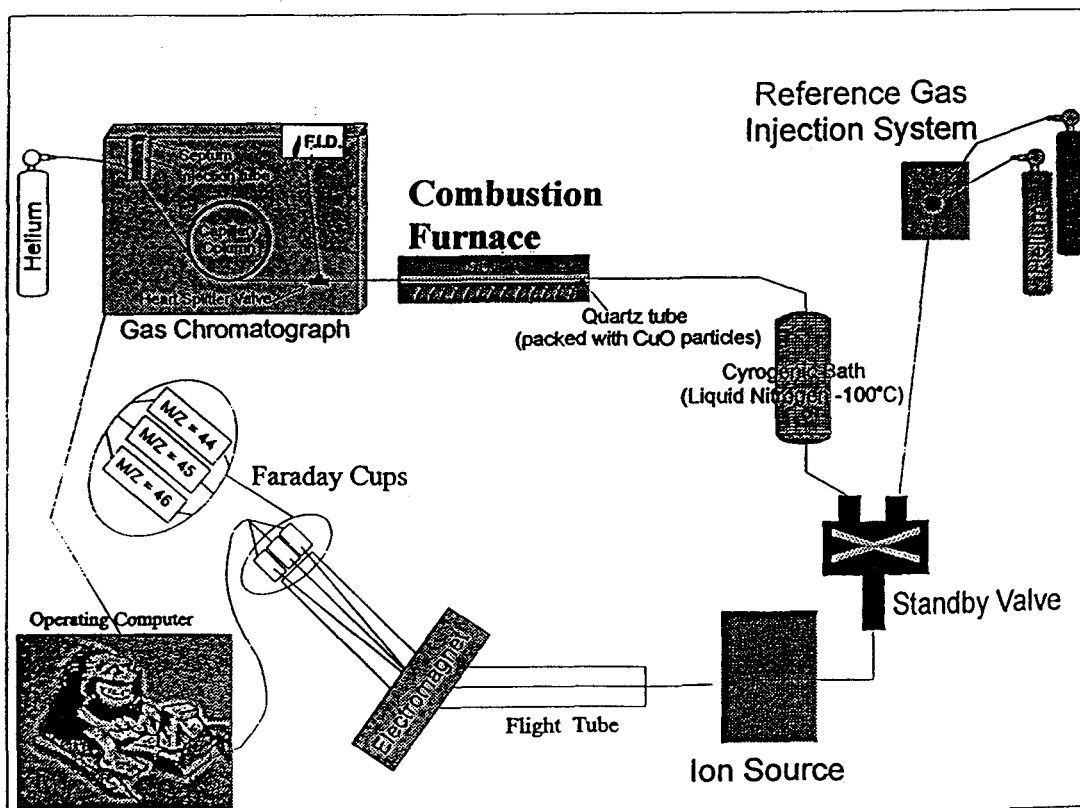
Sampling begins by first inserting the metal tube into the wood cuttings to a depth of 10 cm. The first syringe (the purge) is then used to evacuate all atmospheric gases from the metal tube. Next, the stopcock is turned to connect the second syringe to the metal tube, and a 60 cc gas sample is collected from the wood wastes. A clamp on the connecting tube locks the sample into that syringe. The stopcock is turned toward the purge and the sampling syringe is removed, allowing the purge to be emptied into the air. Another sampling syringe is put in place and the metal tube is inserted another 10 cm into the organic cover. The purge syringe is used to remove gases from the previous sampling level, then the stopcock is turned to the sampling syringe. This process is repeated to a depth of 150 cm (the length of the metal tube), or until the tip of the metal tube enters into a zone saturated with water.

Sampled gases were transferred into 15 ml glass vials closed by plastic caps containing a 0.125" thick Silicon/Teflon septum. That storage method was adapted from procedures used in other stable isotope labs for keeping gas samples for a prolonged period of time without isotopic fractionation (*e.g.* University of Waterloo, Robert Drimmie and Edward Hornibrook, personal communication; University of Toronto, Barbara Sherwood-Lollar and Niel Arner, personal communication). First, a vial and the tip of a sampling syringe are submerged into distilled water. The clamp closing the syringe is opened, and the gas sample is transferred under water into the upside-down vial, displacing the water that fills the vial to its mouth. The cap is screwed below the water surface, preventing any loss or contamination with atmospheric gases. All vials are stored upside-down, at 4 °C, the cap under water, until analysis.

2.2 ISOTOPIC ANALYSES (GC-C-IRMS)

Carbon isotope composition was determined by Gas Chromatography-Combustion-Isotopic Ratio Mass Spectrometry (GC-C-IRMS; Figure 3). This analytical system separates the gaseous or volatile constituents of a bulk sample into individual components by chromatography. The separated gases are then carried first into a combustion furnace, where their carbonaceous components are converted to carbon dioxide. The gases then passed through a cryogenic bath (-100°C) where other gases are condensed. The CO_2 derived from each gaseous component finally arrived in turn in a conventional isotopic ratio mass spectrometer, for determination of isotopic ratios.

Figure 3. The GC-C-IRMS System.



2.2.1 Gas Chromatography

Gas separation was performed on a Hewlett Packard 5890 Series II Gas Chromatograph (GC) equipped with a Chromopack, PoraPlot-Q fused silica, capillary column (25 m x 0.27 mm i.d.). This type of column offers good separation of methane, carbon dioxide and other light substances in a relatively short time period. Table A-1 in Appendix A outlines the procedure followed during trials completed to maximize separation of component gases. Best separation was achieved at the following GC operating conditions:

- Oven temperature: Room temperature (25-28°C);
- Carrier Gas: Helium;
- Column Head Pressure: 10 psi;
- Flow rate: 20 ml/min;
- Injector Temperature: 250°C;
- Detector Temperature: 250°C.
-

These conditions were subsequently retained for all further isotopic analysis. Run times for sample analysis were less than six minutes. Retention times for methane were approximately 215 seconds, while those for carbon dioxide were approximately 250 seconds.

2.2.2 Combustion and Injection Concentrations

One important concern when measuring the carbon isotope composition of gas mixtures containing methane is whether or not 100% of the methane is converted to carbon dioxide in the combustion furnace. Merritt *et al.* (1995) observed an isotopic

fractionation when the combustion furnace was set at a temperature inferior to 900°C and/or when the amount of methane in the injected sample exceeded 5 nmol/vol.

In order to test if quantitative methane oxidation did occur in our analytical system, two trials at 850°C and two trials at 900°C were completed using two types of carbon dioxide, methane and inert gas mixtures. The first contained 9.98% methane and 90.02% argon, while the second mixture contained 5% methane, 5% carbon dioxide and 90% helium. The mixtures were transferred into 15 ml glass vials similar to those used for field samples, as described in Section 2.1. For all trials, injections of 40 μ l samples were completed using a Hamilton SL-120 "sample lock" gas tight syringe. Ten injections were completed during each trial. The detailed results are listed in Tables A2-A5 (Trials A to D), in Appendix A.

Isotopic precision for methane, expressed as the standard deviation for the obtained $\delta^{13}\text{C}$ results during Trials A and C (combustion furnace temperature = 850°C), were in both cases $\pm 0.4\%$. Similar values for Trials B and D (combustion furnace temperature = 900°C) were in both trials $\pm 0.3\%$. It follows that precision is not significantly affected by methane concentrations lower by a factor of 2, with a similar amount of carbon dioxide. However, a 50°C difference does matter. As a result, subsequent isotopic analyses were completed at 900°C, due to the fact that this combustion temperature offers better precision and is in agreement with previously successful scientific procedures.

2.2.3 Mass Spectrometry

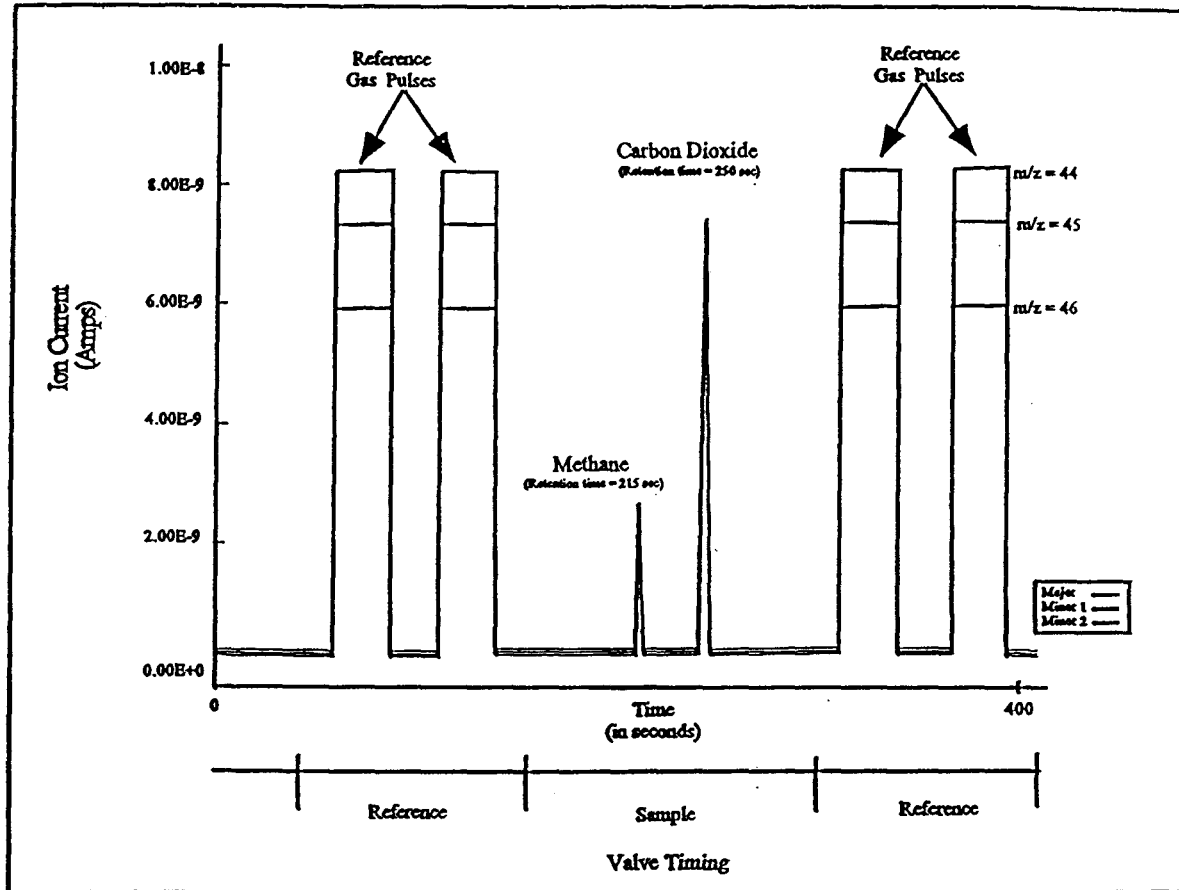
Isotopic analyses were completed on a Fisons Isotech Prism III, isotope ratio mass spectrometer. This type of mass spectrometer is equipped with four collectors, two of which were set at mass/charge (m/z) 44 and 46. A third collector is permanently set at

m/z 45. For carbon dioxide, mass 44 represents $^{12}\text{C}^{16}\text{O}_2$, mass 45 represents $^{13}\text{C}^{16}\text{O}_2$ and mass 46 represents $^{12}\text{C}^{18}\text{O}_2$. The $\delta^{13}\text{C}$ value for a measured gas is obtained from a ratio of masses 44 and 45, using the internationally accepted equation:

$$\delta^{13}\text{C} = \left[\left(\frac{^{13}\text{C}}{^{12}\text{C}} \right)_{\text{sample}} - \left(\frac{^{13}\text{C}}{^{12}\text{C}} \right)_{\text{reference}} \right] \div \left[\left(\frac{^{13}\text{C}}{^{12}\text{C}} \right)_{\text{reference}} \right] * 1000 \quad (\text{Eq. 5})$$

A calibrated research grade carbon dioxide gas, automatically injected into the mass spectrometer, served as the internal reference. Reference pulses occurred twice before and twice after each gas sample. The $\delta^{13}\text{C}$ of sample gases were then subsequently calculated relative to this reference gas, which has an isotopic value of -21.32‰ relative to the international standard NBS-19 (PDB). All isotopic corrections including the correction for the presence of ^{17}O (Craig, 1957) were performed automatically by the operating computer. Figure 4 demonstrates a typical chromatogram obtained during GC-C-IRMS analysis.

Figure 4. Typical chromatogram obtained in GC-C-IRMS analyses.



As each pulse is obtained from the same source, the reference pulses obtained during each run should in principle have the exact same isotopic value. Consistency of the values obtained from the readings of these reference pulses is considered to reflect the system stability. In order to verify that the system is stable and functioning with an acceptable margin of error, a system stability ratio (SSR) is calculated from the readings obtained following analyses of the reference pulses. The SSR is calculated by dividing the reading obtained in Collector 1 ($m/z = 44$) by the reading obtained in Collector 2 ($m/z = 45$). In practice the $\delta^{13}\text{C}$ values obtained from analyses of sample gases may only be considered as valid when the system stability ratio is inferior to 5.0×10^{-7} .

At the beginning and end of each day, as well as periodically throughout the experiment, stability tests consisting of ten pulses of the fore-mentioned carbon dioxide reference gas were completed. All results indicating a system stability ratio higher than this accepted value were excluded from the study and further trials were not completed until the desired system stability level had been reached. As described in Table A-6 (Appendix A), the average stability ratio value for all analyses, including laboratory trials was 3.1755×10^{-7} .

Another important concern when completing isotopic analysis is the linearity of the mass spectrometer. As described in the operator's manual, the isotopic linearity for a mass spectrometer of this design is only guaranteed when the concentration ratios of the injected component gases are above a specified threshold. In the case of bulk samples including carbon dioxide and methane, the ratio is 20:1. All samples analysed during this study fall within acceptable ranges for these values and isotopic linearity of the mass spectrometer was therefore guaranteed.

2.2.4 Precision and Reliability of Results

Sensitivity of isotopic results to multiple piercing of septums attached to sample vials was tested by comparing analyses from multiple vials to multiple analyses from a single vial (Laboratory Tests E, Table A-7, Appendix A: seven analyses using seven different vials, each one with a new septum that was pierced only once for $\delta^{13}\text{C}$ determination; Laboratory Tests F, Table A-8, Appendix A: same vial pierced on ten different occasions). Results demonstrate that the analytical precision is the same (standard deviations of 0.3 for methane and 0.2 for carbon dioxide), and that the reliability of the analyses was not compromised by repeated sampling of the same vial.

Proper performance of the GC-C-IRMS system over 10 days of analytical work, as well as the daily performance, was checked by analysing each day a different vial of a gas mixture of known composition and isotopic signature. Table A-9 (Appendix A) gives the detailed results for the 87 analyses performed before, during and after sample analysis. The daily mean was varying irregularly, from a high of -17.1‰ to a low of -19.1‰ (overall average of -17.9‰, with a standard deviation of 0.6). However, all of the daily $\delta^{13}\text{C}$ standard deviations were acceptable (0.3 or better), pointing to a possible isotopic fractionation from one vial to the other, rather than an improper functioning of the instruments.

CHAPTER 3

RESULTS

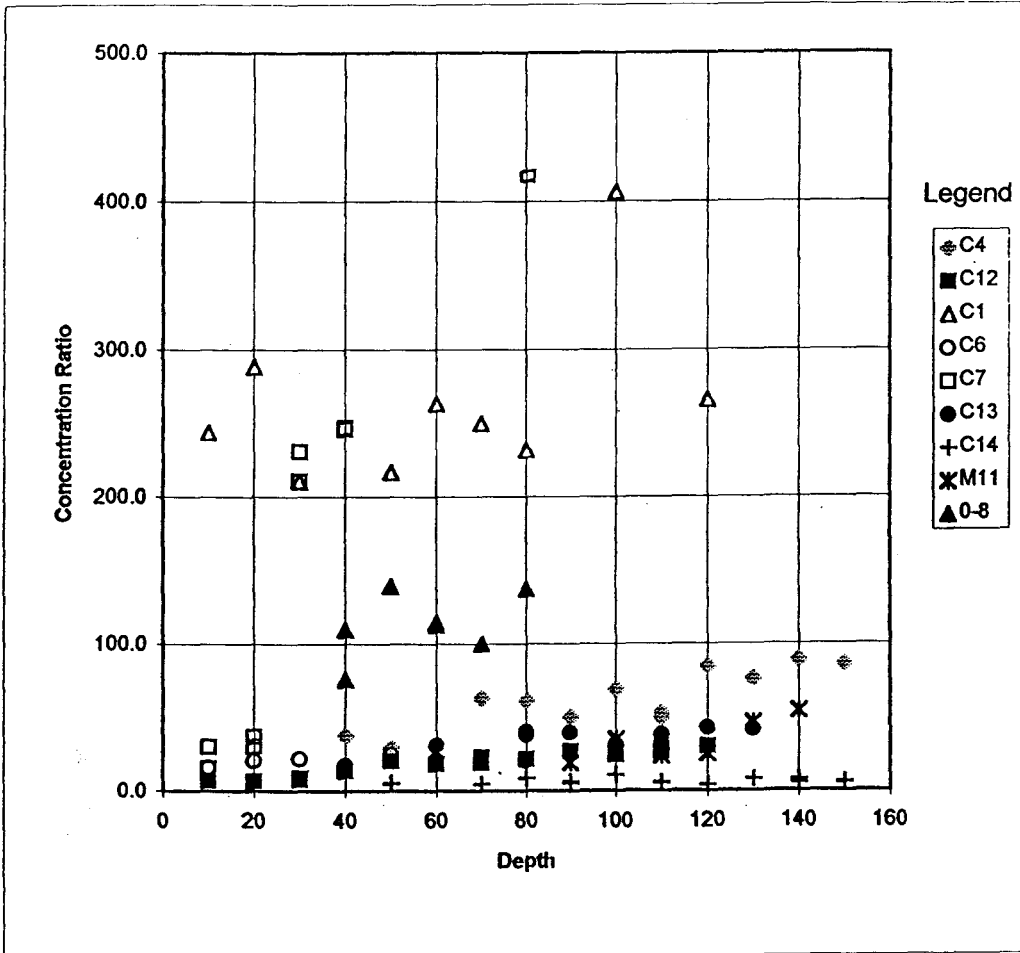
3.1 METHANE/CARBON DIOXIDE CONCENTRATION RATIOS

A general account of the pore gas content of the wood wastes at East Sullivan is provided by Tassé *et al.* (1994), Tassé and Germain (1996), Tassé *et al.* (1997). In these studies, oxygen, starting from a 22% atmospheric level, is generally consumed within the top 50-70 cm of the organic cover. Consumption occurs mainly as a result of carbon oxidation. As a result, carbon dioxide increases in proportions inverse to oxygen decline. Concentrations up to 51%, well above the maximum predicted by the stoichiometric oxidation of carbon (22%), were noted. That "excess CO₂" is probably related to methanogenesis which releases both carbon dioxide and methane when fermentation occurs (see next chapter). Methane is found in proportions that vary from trace amounts to 60%, according to sample depth and location. Roche Ltée (1994) also reports on interstitial gases sampled in experimental plots surveyed over two years. In that case, no significant difference was noted between the experimental plots and the natural cover.

Although the exact concentrations of carbon dioxide and methane can not be identified through the use of the GC-C-IRMS system employed for analyses during this study, it is possible to compare the relative amounts of methane and carbon dioxide through analyses of the peak areas obtained for each gas. A "Concentration Ratio" may be obtained by dividing the area under the ion-current peak associated with methane by the equivalent for carbon dioxide and multiplying that value by 100. A concentration ratio of 100 therefore represents equal quantities of methane and carbon dioxide, while a value over 100 indicates a higher concentration of methane than carbon dioxide. The concentration ratios of carbon dioxide and methane for all samples included in this study are presented in relation to sample depth in Figure 5. The readings obtained for individual

samples have been grouped by station and are presented according to sample depth in Tables B1-B14, Appendix B.

Figure 5. Depth profiles of CH₄/CO₂ concentration ratios in pore gases.



Concentration ratios vary from 0 (no methane detected) to 625 (methane 6.25 times more abundant than carbon dioxide). Concentration ratios vary according to wood waste age, site location and sampling depth.

A relationship between the age of the wood waste and the relative abundances of bio-gases is best depicted by Table 2, which lists the concentration ratios observed at 0.5 m for all sampling stations and the average ratios calculated for the four categories of wood wastes to which they pertain. The concentrations ratios are the highest, except for one station (M7), in wood wastes deposited before 1990. They are low or equal to zero in all stations located in wood wastes deposited between 1992 and 1996. Data is insufficient to detail a more precise relationship between the proportions of methane measured in the organic cover and the age of the forest residues or to indicate a difference between coniferous and mixed coniferous/deciduous residue types. It is clear that the highest concentrations of methane are present in the oldest wood wastes. This is true despite the fact that methane is not ubiquitous in these ancient residues.

Table 2. Average values of CH₄/CO₂ concentration ratios at 0.5 m, according to age and type of wood wastes. *Italic and underline*: spot sample. *Normal*: vertical profile. *Subscript*: concentration ratio at station.

Type of Wood Wastes and Year of Deposition	Stations Ranked by Decreasing Ratio	Average Concentration Ratio at 0.5 m
1A, 1984-1990	<i>C2₆₂₅</i> , <i>C0₅₂₂</i> , <i>C5₂₈₆</i> , <i>C7₂₄₆</i> , <i>C1₂₁₆</i> , <i>0-8₁₃₉</i> , <i>C3₉₄</i> , <i>C4₂₉</i> , <i>M7₀</i>	240
1C, 1994-1996	C14 ₅ , C15 ₀	3
2A, 1992-1994	C6 ₂₄ , C13 ₂₀ , M11 ₀ , <i>P5₀</i> , P4 ₀	9
2B, 1994-1996	C12 ₂₁	21

The lowest concentration ratios noted amongst the 1990, Type 1A, wood wastes (C4, C3, 0-8: <150; Table 2), correspond to near-slope/margin locations (Figure 1). Such a setting probably favours inward oxygen diffusion and convection that oxidizes the methane that diffuses outward. This setting therefore compromises to some extent the full anaerobic conditions required for methanogenesis. Oxygen diffusion into the wood wastes is also probably involved at Station M7, which is located far from the margins, but next to a, likely, gas-permeable gravel road. The low concentration ratios in Type 2A deposits are also possibly related to similar causes (M11: site margin; P5 and P4: experimental patches, as mounds over the tailings; Figure 1, Table 2). By extension, it is possible that the low concentration ratios observed within ≥ 1992 wood wastes are partly due to a low compaction that also favours inward diffusion.

Lack of significant amounts of methane was demonstrated over the entire gas profiles measured at C15, M7, M11 and P4, down to 0.6, 0.7, 0.8 and 1.5 m, respectively. However, concentration ratios are also depth-related. Methane was detected below 0.8 m at M11, with a concentration ratio as high as 54 at the bottom of the profile (1.4 m). Concentrations of methane relative to carbon dioxide generally increase with depth, with a significant rise below 0.2-0.4 m (Figure 5). For example, Station C7, which is located in the northwest corner of the study site (Figure 1), shows a concentration ratio which averages 25 in the top 0.2 m. This ratio value increases to 210-250 at 0.3-0.4 m, and over 17 times to 420 at a depth of 0.8 m. At Station C12, differences between depths are less drastic, but the general tendency remains the same. In the top 0.3 m of the wood waste cover, the concentration ratios average 7, while at 1.20 m, the concentration ratio is 30. Similar tendencies have been noted for Stations C1, C4, C13 and M11. However, no such trend is present in the results for Stations C14 and 0-8, which are located along the limits of the organic cover. C6 is exceptional in that methane was detected only in the upper 0.8 m, and missing below that depth.

3.2 CARBON ISOTOPE RATIOS OF METHANE AND CARBON DIOXIDE

The results of carbon isotope analyses for both carbon dioxide and methane extracted from all sampling stations are presented graphically in Figures 6 and 7, as well as numerically and as individual depth profiles in Appendix B (Tables B1-B14; Figures B1-B13).

The isotopic ratios of carbon dioxide ($\delta^{13}\text{C}_{\text{CO}_2}$) are restricted to a field of variation which is much narrower than the equivalent field of variation observed for methane. Overall, the carbon isotope ratios obtained for carbon dioxide vary between -24‰ and -10‰ (Figure 6), whereas values for methane vary between -75‰ and -20‰ (Figure 7).

$\delta^{13}\text{C}_{\text{CO}_2}$ profiles are generally smooth. Only a few profiles show outliers 4‰ to 6‰ outside the general trends (*e.g.* C4, in Figure 6, and C1 and C7). Isotopic ratios gently increase with depth, with gradients that vary generally between 0 and 5‰/m, but can be as high as 17.5‰/m in short profiles (C7, C15, M7, 0-8: ≤ 0.8 m; Table 3). Large gradients can also be observed in the upper part of some deep profiles (C4 and C13: around 8‰/m, above 0.7-0.8 m; Table 3). Averages $\delta^{13}\text{C}_{\text{CO}_2}$ calculated for samples at 0.7 m and deeper, that is, in the low-gradient parts of the profiles, spans only 9.1 δ -units, from -19.3‰ to -10.2‰. Carbon isotopes seem to be heavier in older wood wastes, between -10‰ and -16‰, compare to -16‰ to -19‰, but that must be considered as a tendency rather than a strong statement, given some overlap in the $\delta^{13}\text{C}_{\text{CO}_2}$ distribution (Figures 6 and 8).

Figure 6. Depth profiles of isotopic results for carbon dioxide. All samples, with line drawing for typical profiles (C12: normal; M7: short, high gradient; C4: long, with elusive break in gradient in the upper part, and an outlier at 0.3 m; 2E-8: wood waste free station).

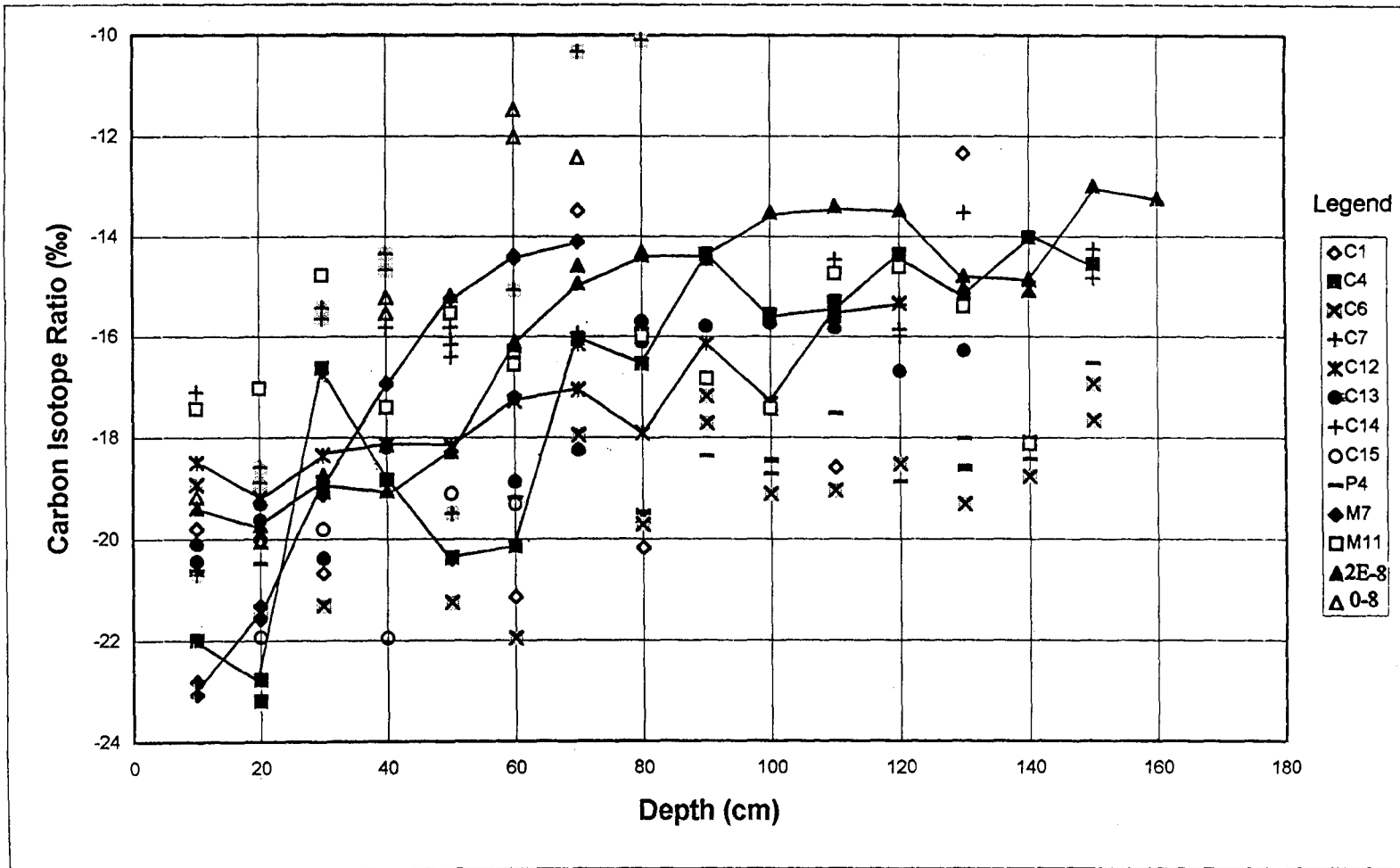


Figure 7. Depth profiles of isotopic results for methane. All samples, with line drawing for typical profiles (C7: normal; C13: without methane at shallow depth; C12: inverse gradient).

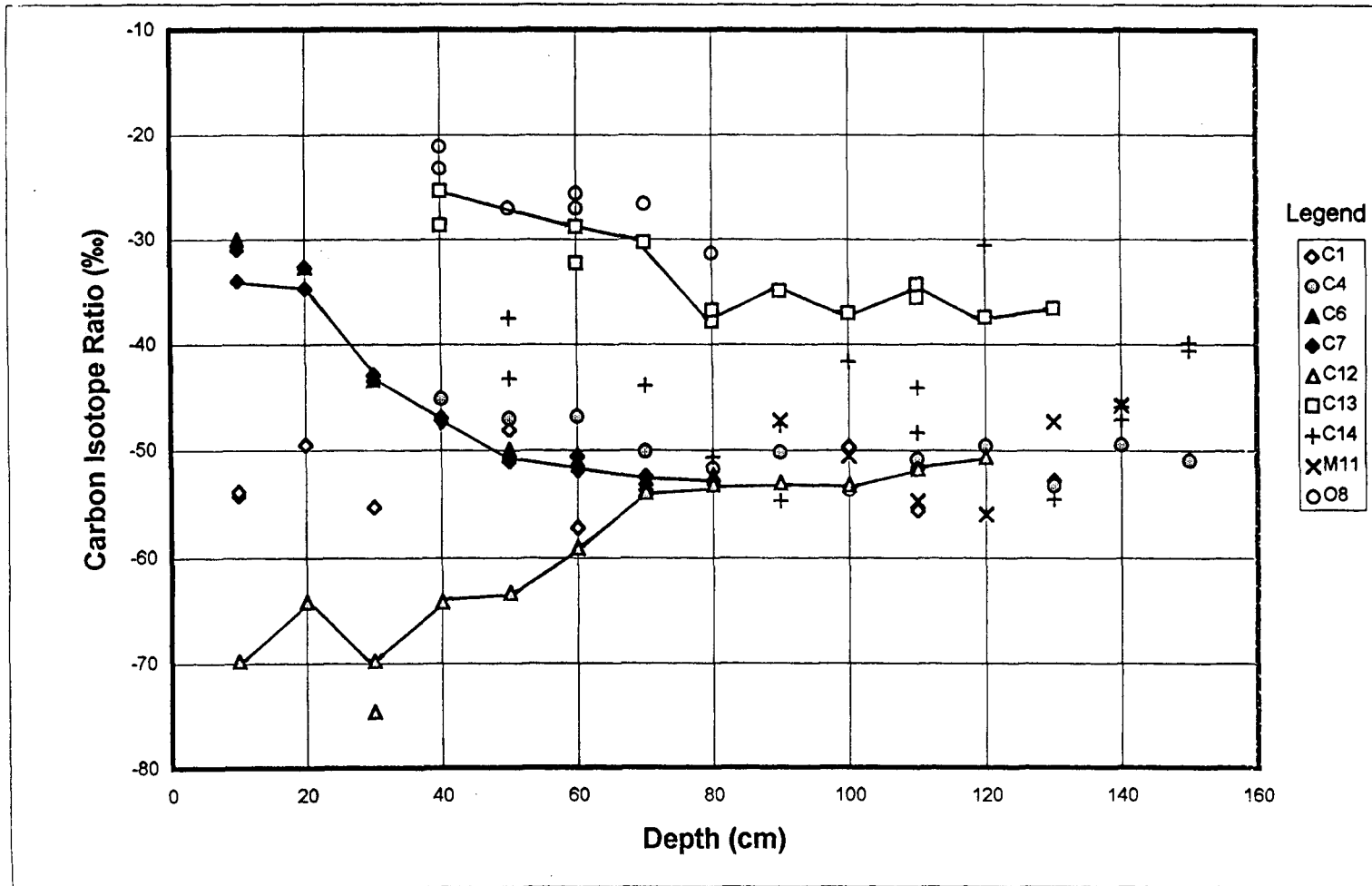


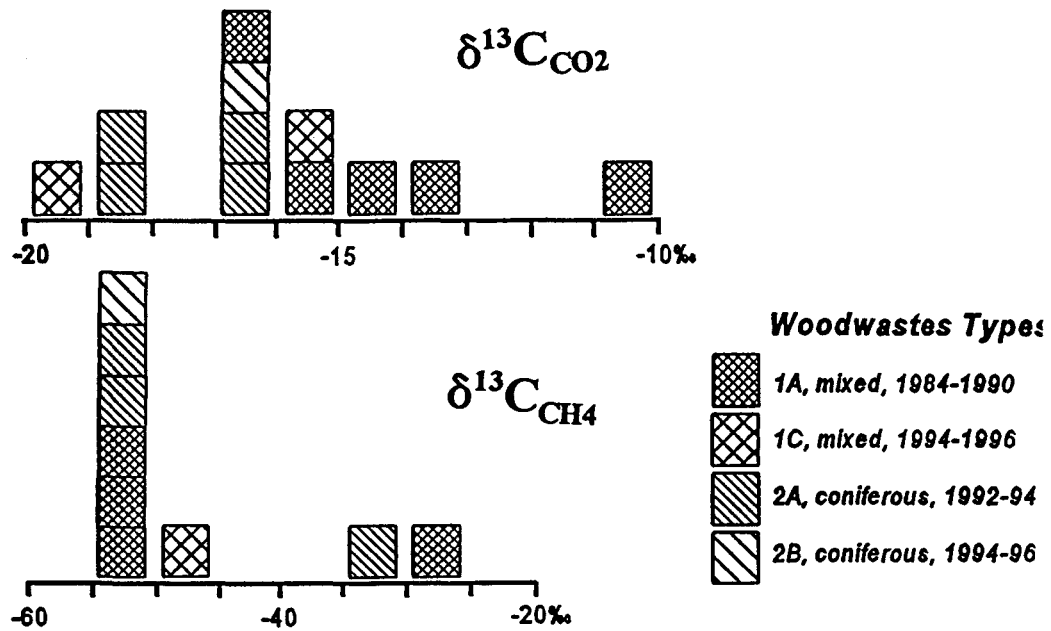
Table 3. Summary of $\delta^{13}\text{C}_{\text{CO}_2}$ and $\delta^{13}\text{C}_{\text{CH}_4}$ results as average values and trends, for each station sampled.

Wood Waste Type	Profile	Length m	$\delta^{13}\text{C}_{\text{CO}_2}$ gradient ‰/m^*	$\delta^{13}\text{C}_{\text{CO}_2}$ ‰^{**}	$\delta^{13}\text{C}_{\text{CH}_4}$ gradient ‰/m^*	$\delta^{13}\text{C}_{\text{CH}_4}$ ‰^{**}
1A	C1	1.5	4.3	-16.2	0.0	-53.0
1A	C4	1.5	above 0.8 m: 8.8 below 0.8 m: 2.5	-15.2	-16.3 0.0	-51.1
1A	C7	0.8	13.8	-10.2	above 0.5 m: -50.0 below 0.5 m: -6.3	-52.8
1A	0-8	0.8	13.8	-13.4	-19.5	-29.1
1A	M7	0.7	17.5	-14.1	--	N.D.
1C	C14	1.5	2.1	-15.2	0.0	-45.1
1C	C15	0.6	6.7	-19.3	--	N.D.
2A	C6	1.5	1.9	-18.5	above 0.5 m: -50.0 below 0.5 m: -7.7	-53.0
2A	C13	1.3	4.3	-16.3	above 0.8 m: -25.5 below 0.8 m: 1.6	-31.2
2A	M11	1.4	0.0	-16.2	-15.6	-50.2
2A	P4	1.5	2.1	-18.3	--	N.D.
2B	C12	1.2	2.9	-16.5	above 0.7 m: 32.2 below 0.7 m: 6.6	-52.6
Tailings	2E-8	1.6	above 0.7 m: 7.5 below 0.7 m: 1.0	-14.0	--	N.D.

* : estimated by visual regression; a positive gradient means increasing downward $\delta^{13}\text{C}$ values.

** : average of ≥ 0.7 m $\delta^{13}\text{C}$ values.

Figure 8. Distribution of average $\delta^{13}\text{C}_{\text{CO}_2}$ and $\delta^{13}\text{C}_{\text{CH}_4}$ and relation with age and type of wood wastes.



The $\delta^{13}\text{C}_{\text{CO}_2}$ profile measured at Station 2E-8, within tailings, in an organic-free environment, shows trends similar to those observed in the wood waste cover. Isotopic ratios increase downward, rapidly near the surface at depths ranging between 0.4 m and 0.7 m and more slowly at depth (Figure 6; Table B-13). In that case, carbon dioxide is released from pore water as a result of acid-neutralization reactions with carbonate minerals (Germain *et al.*, 1992). Nevertheless, $\delta^{13}\text{C}_{\text{CO}_2}$, at -14.0‰, is comparable to average values noted in the wood waste bio-gas.

$\delta^{13}\text{C}_{\text{CH}_4}$ depth profiles are also generally smooth, with some outliers 10‰ to 15‰ outside the general trends (*e.g.* C7). As noted for carbon dioxide, the higher gradients are observed in the surficial samples, but contrary to carbon dioxide, isotopic ratios become less negative with depth. The most negative isotopic ratios are reached in profiles where methane is detected close to the surface (C6 and C7: -50.0‰/m). C12 is exceptional in that $\delta^{13}\text{C}_{\text{CH}_4}$ decrease with depth, with a gradient of 32.2‰/m. Isotopic ratios for methane are almost invariant at depth, despite the large variations observed in superficial zones. Gradients vary around zero, with extreme excursions at -7.7‰/m and +6.6‰/m (Table B-1 to B-14). Average $\delta^{13}\text{C}_{\text{CH}_4}$ values calculated for samples at 0.7 m and deeper, vary considerably, from -53.0‰ to -29.1‰. However, only 2 of these results are around -30‰ (0-8 and C13), whereas the 7 others cluster around -50‰ (Figure 7). Heavy $\delta^{13}\text{C}_{\text{CH}_4}$ values are found in sewage-free areas, while other sewage-free sampling sites are characterised by light isotopic carbon (*e.g.* C6, C12). No relationship can be made between either the age or type of wood wastes, the location on the organic cover, or the presence/absence of raw sewage in the area of the sampling station.

It follows from these observations that methane appears to be more prone to large isotopic fractionations than does carbon dioxide. Moreover, the isotopic fractionations of the bio-gases and their related reactions appear to dominate to a much larger degree in superficial areas of the organic cover than at greater depth. For the

purpose of discussion, the organic cover is thus considered to be comprised of two distinct units. The first unit (Zone A) encompasses wood wastes between the surface and depths of approximately 0.5 m to 0.8 m. The second unit (Zone B) is located between Zone A and the water table or the base of the organic cover. As previously mentioned, these units match the aerobic and anaerobic profiles in the portion of the organic cover which is located above the water table.

CHAPTER 4

DISCUSSION

4.1 BIOGENIC GASES AND METHANOGENESIS

Carbon dioxide and methane are well known products of wood-waste degradation (*e.g.* Reardon and Poscente, 1984; Tassé *et al.*, 1994). Carbon dioxide is the result of the oxidation of organic matter, commonly by molecular oxygen, as shown by the reaction:



Carbon oxidation can also occur in anaerobic environments, when other oxidants are available. For instance, Froelich *et al.* (1979) provides a model of organic matter oxidation which uses, in turn, O_2 , MnO_2 , HNO_3 , Fe_2O_3 and SO_4^{2-} , in a mineral matrix in which these components are available. The succession is dictated by the Gibbs free energy (ΔG°) involved in the reactions, oxidation using the oxidant which involves the lowest energy, from O_2 to SO_4^{2-} (-3190, about -3090, -2750, about -1410, and -380 kJ per mole of glucose, respectively; ΔG° also varies according to MnO_2 and Fe_2O_3 mineralogy). When a given oxidant is no longer available, oxidation continues, using the next reducible molecule for which the reaction has the lowest ΔG° value. This process continues until all oxidants (or all organic matter) are consumed. Methanogenesis follows, with its high ΔG° (-350 kJ per mole of glucose). It is a terminal step in biogenic organic matter degradation.

4.2 METHANOGENIC PRODUCTION PATHWAYS

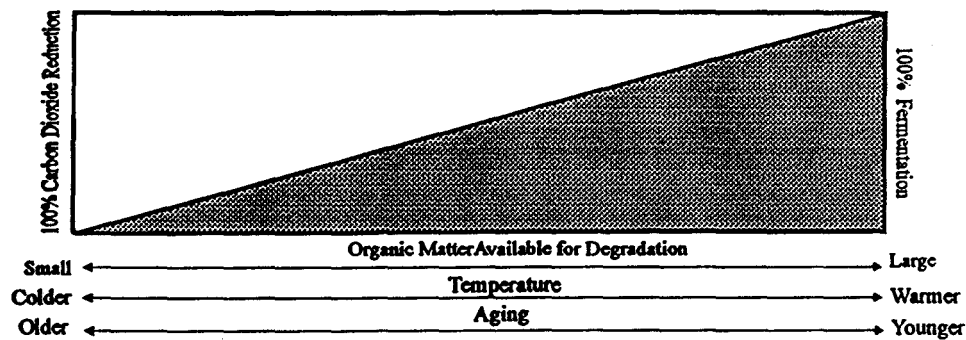
Since the recognition of the Greenhouse effect as an environmental problem, much research has been undertaken on the subject of methanogenesis. This research has led to an increased knowledge of the mechanisms by which methane is produced and the ways by which it reacts once present in the terrestrial environment. Biogenic methane is produced through two primary pathways involving bacteriologically mediated reactions (Schoell, 1988). These two pathways are fermentation and CO₂ reduction. Fermentation produces methane and carbon dioxide, as methyl groups of substrates of acetate, methanol, methylated amines, organic acids (Equation 7) etc., are hydrogenated (Pine and Baker, 1956 in Whiticar *et al.*, 1986). As a result of the co-generation of CH₄-CO₂, fermentation can increase the CO₂ concentrations above those derived from carbon oxidation solely. Biogenic methane produced in freshwater sediments where fermentation is the major production pathway is characterised by a depletion in both ¹³C and deuterium (D) ($\delta^{13}\text{C} \sim -65\text{‰}$ to -50‰ , $\delta\text{D} \sim -400\text{‰}$ to -250‰ ; Whiticar *et al.*, 1986). Conversely, CO₂ reduction (Equation 8) involves a reaction between carbon dioxide and hydrogen. Methane from marine sediments where CO₂ reduction is the dominant pathway is even more depleted in ¹³C, but less depleted in D ($\delta^{13}\text{C} \sim -110\text{‰}$ to -60‰ , $\delta\text{D} \sim -250\text{‰}$ to -170‰ ; Whiticar *et al.*, 1986). A more in-depth and precise description of these processes is provided by Schoell (1980), Whiticar *et al.* (1986), Schoell (1988) and Hornibrook *et al.* (1997).



CO₂ reduction and fermentation may act simultaneously in the production of methane, although the proportions and importance of each chemical process changes from source to source, depending upon the conditions of the individual system (Whiticar *et al.*, 1986; Hornibrook *et al.*, 1997). Reports of these pathways are numerous, but a clear

understanding of their occurrence as yet to emerge (Hornibrook *et al.*, 1997, and references therein). Since the dominating pathway seems to be independent of the depositional environment, whatever the location of biogenic methane production in the Earth's crust, Schoell (1988) proposed that the predominance of one or the other pathway is basically governed by the availability of organic matter in the substrate and environment temperature (Figure 9).

Figure 9. Relative degree of importance of each of the methanogenic production pathways (modified from Schoell, 1988)



With respect to the East Sullivan site, pore water geochemistry of the organic cover has been shown by Tassé and Germain (1996) to be uniform over the site. This is a result of the fact that the pore water is mainly derived from meteoric infiltration. The water table is usually low within the cover when compared to the wood waste/tailings interface (Tassé and Germain, 1996). Therefore, it follows that the pore water geochemistry of the organic cover is not an important parameter with respect to the determination of the dominant production pathway of methanogenesis.

As far as temperature is concerned, Martens *et al.* (1986) noted that this parameter was a controlling factor on methanogenesis and isotopic fractionation with respect to the determination of the dominant production pathway in a coastal sediment environments. CO₂ reduction tends to dominate colder environments while fermentation gains relative importance as the temperature increases. At East Sullivan, temperature is uniform within the wood waste cover and relatively stable over time. A one year survey at intervals of two weeks showed that the temperature stays above 0°C all year at depths below 0.7 m in the older deposits of the entire cover at depths below 0.7 m (N. Tassé, INRS-Géoresources, personal communication). Moreover, at depths between 1.0 and 3.0 m, the average temperatures only vary between 7.0 and 7.7°C over the entire year. The range of variation narrows with depth, with standard deviations of ±5.0, ±3.0 and ±2.7°C respectively at depths of 1.0, 2.0 and 3.0 m below the surface. Therefore, available information to date indicates that there are no important variations in the temperature within the organic cover. As a result, it is unlikely that temperature plays an important role in the determination of the dominant methanogenic pathway within the wood wastes.

At a given temperature, the amount of metabolizable organic material available for degradation is the major controlling factor. Systems with abundant biodegradable organic matter are dominated by fermentation. As biodegradation progresses, the pool of

available, fresh, reactive organic compounds, becomes progressively depleted. The relative importance of fermentation therefore decreases, because it is directly dependant on the shrinking availability of methanogenic precursors. This is well demonstrated by Hornibrook *et al.* (1997), who described a shift with depth in the methanogenic pathways of two temperate freshwater wetlands. Fermentation dominates areas near the surface, where the normal soil produces labile substrates which are easily and rapidly consumed. CO₂ reduction progressively gains importance in deeper zones, because the amounts of reactive substrates are diminished. This is also in agreement with studies reporting an "aging effect" in different production environments (*e.g.* Jenden and Kaplan, 1986 and Woltemate *et al.*, 1984 in Schoell, 1988).

The question relevant to this study in order to decipher the long term efficiency of the organic cover is therefore not "What are the methane production mechanisms present within the organic cover?", but rather "What is the dominating mechanism of methanogenesis within the system?". Since CO₂ reduction replaces fermentation as the main pathway, with the progressive depletion of reactive organic substrates, the relative importance of these processes will indicate to what extent the organic cover contains enough metabolizable organic materials or "fuels" for oxygen consumption and methanogenesis for the years to come.

4.3 THE DOMINANT METHANE PRODUCTION PATHWAY AT EAST SULLIVAN

As mentioned in the previous section, methanogenesis by fermentation and CO₂ reduction involves different chemical reactions and bacterial processes. As a result, carbon used in these reactions is subject to isotope fractionation. On these grounds, Whiticar *et al.* (1986) compiled a data base of $\delta^{13}\text{C}$ values of both carbon dioxide and methane from reliable sources where the dominant production pathway was known. A cross-plot

diagram of isotopic data gathered from freshwater and marine environments allowed the outline of two specific fields related respectively to fermentation and CO₂ reduction as well as the determination of empirical fractionation factors for each of these fields.

In order to identify the dominant production pathway within the organic cover, data obtained from the East Sullivan site was plotted on a modified version of Whiticar's *et al.* (1986) diagram (Figure 10; individual plots for each station in Appendix B, Figures B14-B22). All samples from Stations C1, C4, C12 and M11 fall within the fermentation zone. However, some samples from Stations C6, C7 and C14, and all samples from Stations C13 and 0-8 plot outside that field. All "spot" samples also plot outside the field. No correlation can be made between the age or type of wood waste for the results falling outside the formal fields. However, it can be noted that they all pertain to the shallow Zone A of the organic cover ("spot samples": 0.5 m; C6 and C7: both 0.1 and 0.2 m), or are from stations located near the limits of the organic cover (C14, 0-8; Figure 1). Moreover, a trend from near-fringe to inner-field results in Whiticar's *et al.* (1986) diagram corresponds to an increasing depth of samples, at Stations C4, C6 and C7 (Appendix B). The only exception is Station C13 which displays no obvious depth or location relationship. This station is however located adjacent to young wood waste deposits. Nevertheless, a trend from shallow to deep samples, towards the field of fermentation, is recognised for Station C13 as well as for Station 0-8.

Figure 11 shows Whiticar's *et al.* (1986) diagram with the data from C13 and shallow and/or near-margin samples removed. Results are clearly condensed within the fermentation field, with only one station, C12, with some points extending towards the CO₂ reduction field.

Figure 10. Cross-plot of $\delta^{13}\text{C}$ for methane-carbon dioxide pairs in the pore gases of the wood waste cover, all samples (diagram modified from Whiticar *et al.*, 1986).

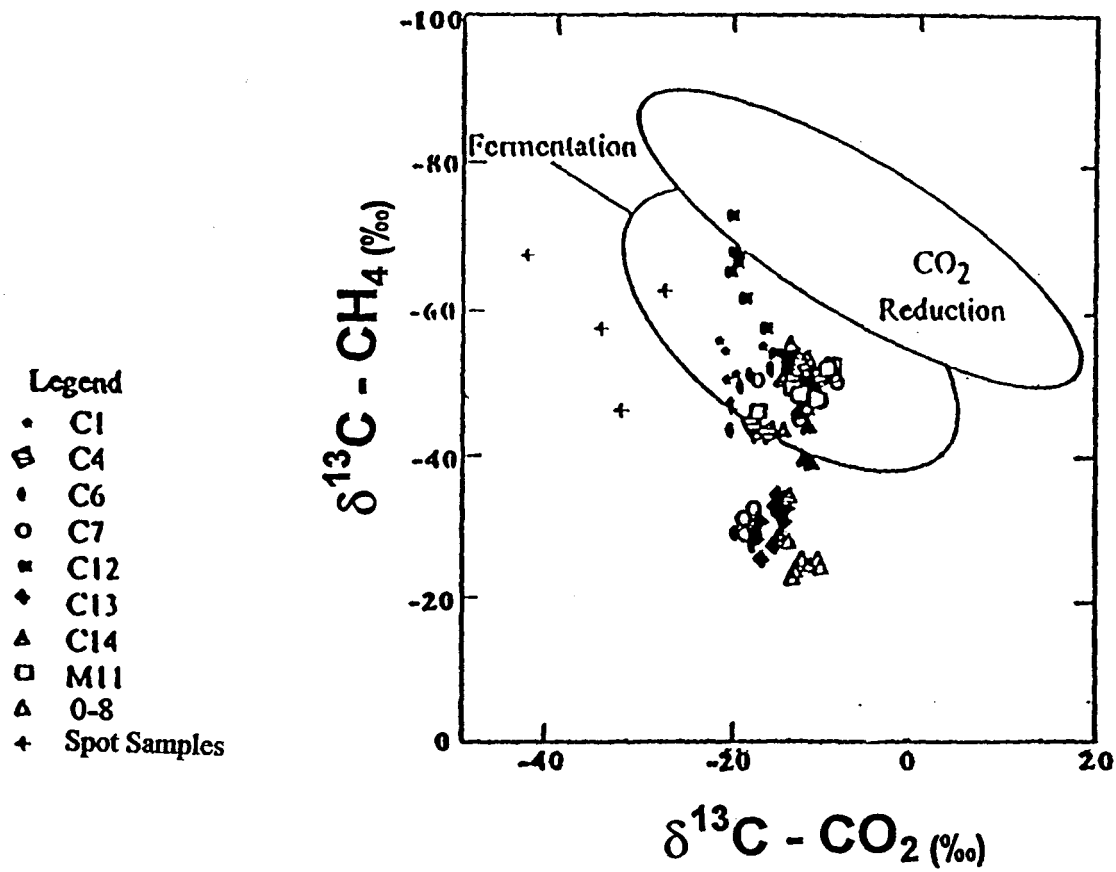


Figure 11. Cross-plot of $\delta^{13}\text{C}$ for methane-carbon dioxide pairs in the pore gases of the wood waste cover, excluding shallow and/or near-margin samples (diagram modified from Whiticar *et al.*, 1986).

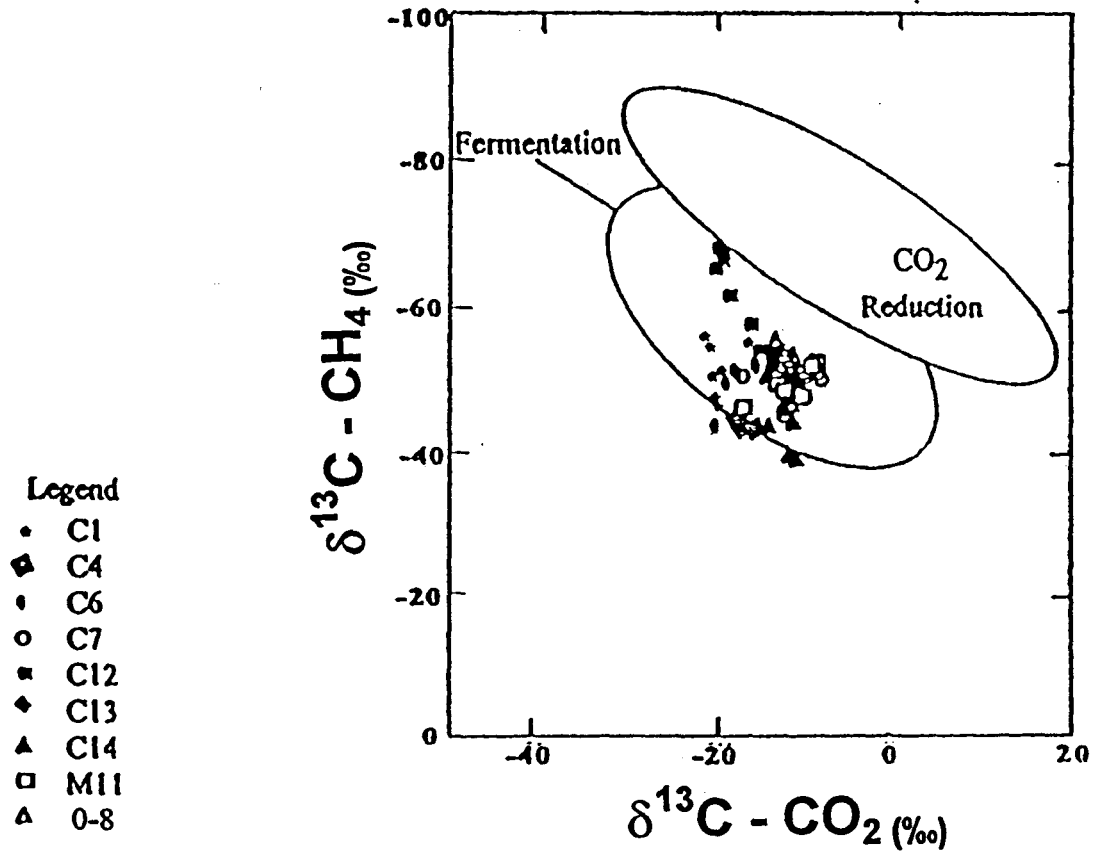
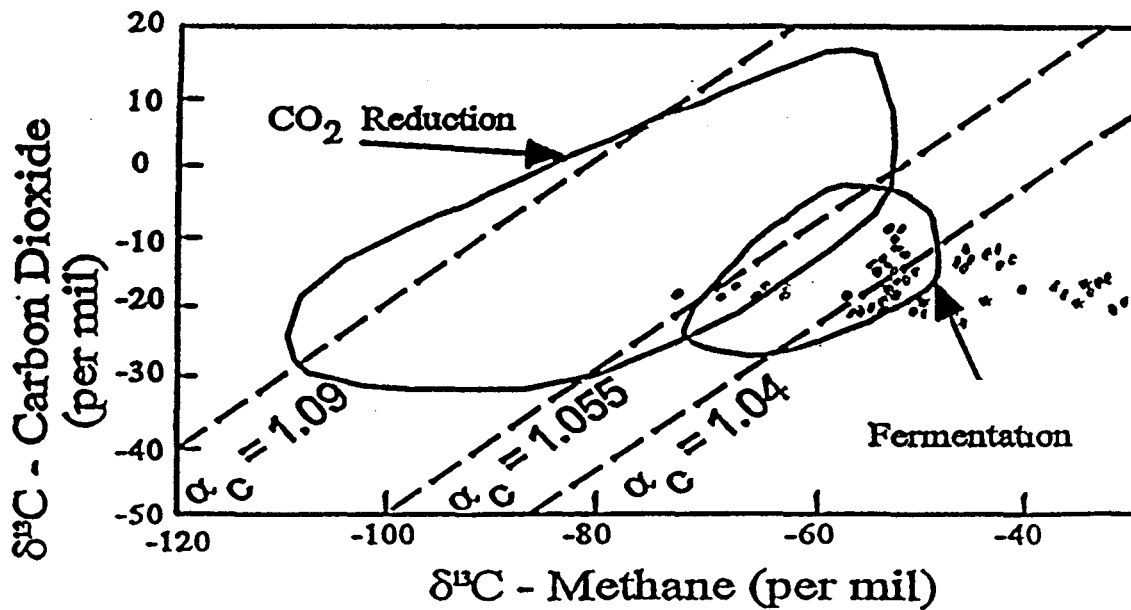


Figure 12 demonstrates how the results from Figure 11 compare to the carbon isotope fractionation factors for coexisting CO_2 and CH_4 produced by fermentation and CO_2 reduction ($\alpha_c \sim 1.040$ to 1.055 and $\alpha_c \sim 1.055$ to 1.090 , respectively; Whiticar *et al.*, 1986). Again, the data are indicated that fermentation dominates the system, with a component of CO_2 reduction for Station C12 being present. Evidence from the carbon isotope composition also suggests that the source of fresh organic matter available for degradation remains plentiful within the organic cover.

Figure 12. Cross-plot of $\delta^{13}\text{C}$ of coexisting CO_2 and CH_4 in pore gases of the wood waste cover (lines are fractionation factors reported by Whiticar *et al.* (1986) to delineate fields characteristic of fermentation [$\alpha_c \sim 1.040$ to 1.055] and CO_2 reduction [$\alpha_c \sim 1.055$ to 1.090]).



Shallow and near margin samples that plot outside Whiticar's *et al.* (1986) fields likely show a fermentation signature obliterated by a process related to air proximity, that is, oxidation by oxygen. Oxygen consumption within the wood waste cover brings oxygen concentration from approximately 22% (atmospheric level) to nearly 0, and favours an inward diffusion at the top of the cover. That mechanism can be accentuated by convection, eventually at deeper levels and near the margins of the cover. Two groups are recognised among the "outsider" samples (Figure 10; Table 4). The main group is characterised by a $\delta^{13}\text{C}_{\text{CH}_4}$ increase, from approximately -40‰ to -20‰, within a bracket of relatively stable $\delta^{13}\text{C}_{\text{CO}_2}$ (C6, C7, C13, C14, 0-8). The other group is related to a $\delta^{13}\text{C}_{\text{CO}_2}$ decrease, from about -20‰ to below -30‰ (C0, C2, C5).

Table 4. General properties of samples plotting outside the fermentation and CO₂ reduction fields.

Station	Sample depth (m)	Nature of $\delta^{13}\text{C}$ shift	Peak area ratio (CH ₄ / CO ₂)
C0	0.5	Low $\delta^{13}\text{C}_{\text{CO}_2}$	522
C2	0.5	Low $\delta^{13}\text{C}_{\text{CO}_2}$	625
C5	0.5	Low $\delta^{13}\text{C}_{\text{CO}_2}$	286
C6	0.1 and 0.2	High $\delta^{13}\text{C}_{\text{CH}_4}$	20.9
C7	0.1 and 0.2	High $\delta^{13}\text{C}_{\text{CH}_4}$	28
C13	0.4 to 1.3	High $\delta^{13}\text{C}_{\text{CH}_4}$	31
C14	1.2	High $\delta^{13}\text{C}_{\text{CH}_4}$	3.8
0-8	0.4 to 0.8	High $\delta^{13}\text{C}_{\text{CH}_4}$	100

Reaction of methane with oxygen produces carbon dioxide (Equation 9). This bacterially driven process preferentially involves light methane ($^{12}\text{CH}_4$) and leaves the remaining methane pool isotopically heavier. Light carbon dioxide ($^{12}\text{CO}_2$) is added into the carbon dioxide pool, which becomes isotopically lighter. Shifts of $\delta^{13}\text{C}$ values similar to those observed at East Sullivan are also reported from other settings and explained by methane oxidation (Coleman *et al.*, 1981; Happel *et al.*, 1994; Hornibrook *et al.*, 1997). The fact that these shifts characterise two different groups at East Sullivan is related to the relative amount of CH_4 and CO_2 in the gas samples. Samples in the group with increased $\delta^{13}\text{C}_{\text{CH}_4}$ are methane poor, with low concentration ratios, whereas samples in the second group are methane rich (Table 4). Consequently, methane oxidation occurring at a given rate will have a large effect on the $\delta^{13}\text{C}_{\text{CH}_4}$ of a methane poor reservoir. A smaller effect will be produced in the second relatively methane rich group. Conversely, a similar rate of oxidation in a methane-rich reservoir will have a small impact on the bulk $\delta^{13}\text{C}_{\text{CH}_4}$ composition, and a much greater effect on the carbon isotope composition of the small amounts of coexisting carbon dioxide.



4.4 PROPOSED MODEL FOR CARBON CYCLE IN THE ORGANIC COVER

Earlier studies of pore gases composition at East Sullivan allowed the recognition of two zones within the organic cover, that is, a shallow zone in which atmospheric oxygen readily diffuses and is consumed by carbon oxidation, and a deep zone where methanogenesis and anaerobic conditions dominate (Tassé *et al.*, 1994, 1997). Isotopic results confirm the presence of these two zones. The shallower zone (Zone A) is characterised by higher gradients of relative CH_4/CO_2 concentrations, $\delta^{13}\text{C}_{\text{CH}_4}$ and $\delta^{13}\text{C}_{\text{CO}_2}$, and extends down to the lowermost point at which atmospheric oxygen is able to diffuse (0.5-0.7 m). The deeper zone (Zone B) extends down to the water table, with no or low gradients (Figures 5 to 7). The depth of the Zone A/Zone B boundary varies

due to the porosity of the wood wastes, the reactivity of the organic matter present and/or the temperature. Figure 13 is a sketch of the carbon cycle in these two zones. That scheme applies to the entire data, except for Station C12, an exceptional case which is discussed in the next section. Atmospheric oxygen diffuses into the wood waste until it is entirely consumed by carbon oxidation in Zone A (Equation 9). Carbon dioxide diffuses upward to the atmosphere, and downward to Zone B, where anaerobic conditions and methanogenesis can add large or small amounts of bio-gas that also diffuse into Zone A and atmosphere (Equations 7 and 8).

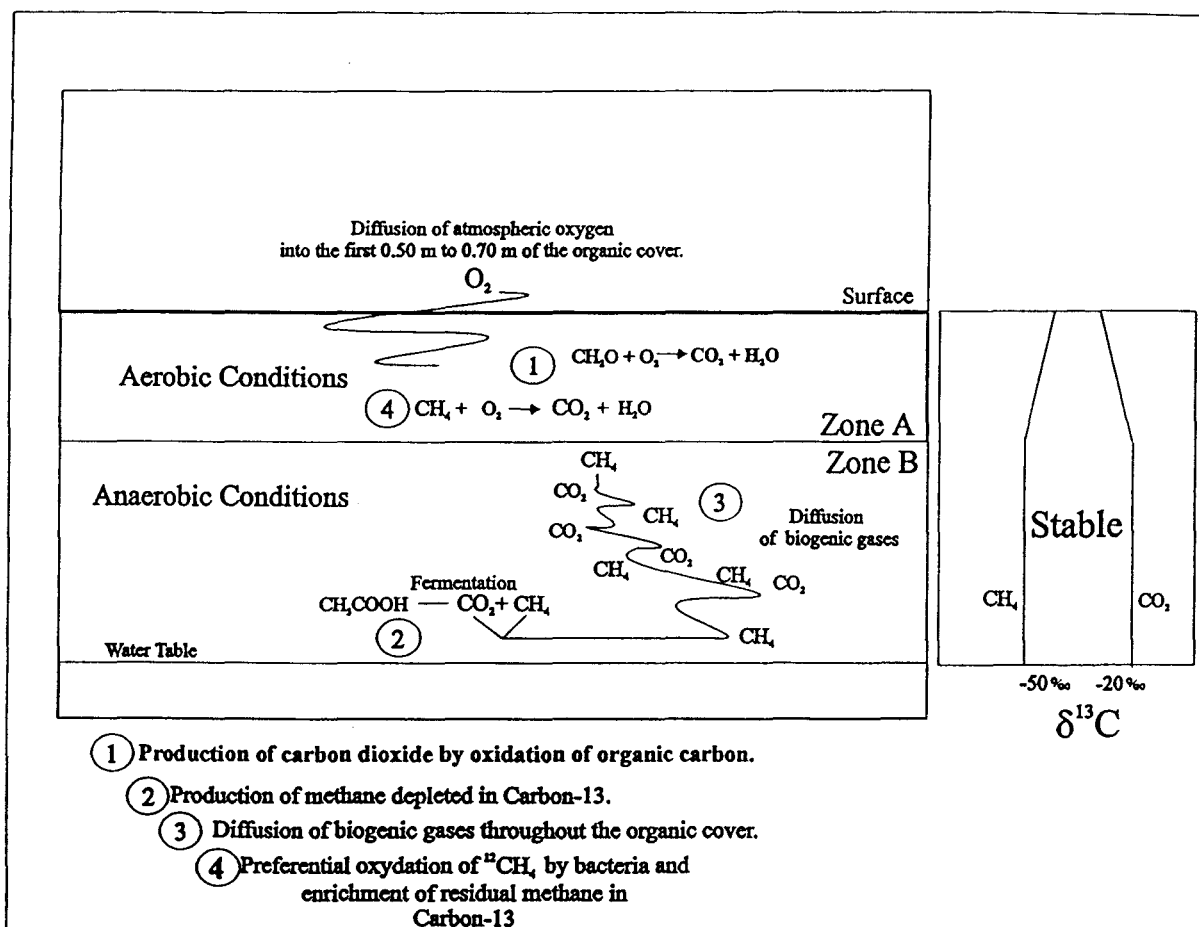
In our profiles, CH_4/CO_2 concentration ratios increase downward, that is, towards the anaerobic zones where methane is generated. Comparison of concentration ratios near the top of zone B show that methane is commonly more abundant within the older wood wastes (≤ 1990) than within the younger ones (≥ 1992) (Table 1). It follows that some degree of decomposition, and not only anaerobic conditions, are required to produce significant amounts of methane. Methane can also be low within old wood wastes, if outward diffusion is favoured by some local factor (*e.g.* proximity to cover margin, or porous gravel road; Figure 1, Table 1). Low compaction of recent wood waste can thus be a factor that enhances the difference in CH_4/CO_2 concentrations between old and young wood wastes.

Carbon isotopic composition varies to a much higher degree for methane than for carbon dioxide (Figures 6 and 7). Gradients for $\delta^{13}\text{C}_{\text{CH}_4}$ are extreme in Zone A, with decreasing trends from $-15\text{‰}/\text{m}$ to $-50\text{‰}/\text{m}$, compare to $0\text{‰}/\text{m}$ to $-8\text{‰}/\text{m}$ in Zone B. $\delta^{13}\text{C}_{\text{CO}_2}$ values increase with gradients that range from $0\text{‰}/\text{m}$ to $18\text{‰}/\text{m}$. Zone A is thus the locus of major isotopic fractionation. Zone B is characterised by low fluctuations and likely best depicts isotopic equilibrium and the nature and isotope compositions of the pore gases as they are produced during wood degradation.

Plots of $\delta^{13}\text{C}_{\text{CH}_4}$ against $\delta^{13}\text{C}_{\text{CO}_2}$ for coexisting gas sampled in Zone B show that methane appears to be produced by fermentation (Figure 11). $\delta^{13}\text{C}_{\text{CH}_4}$ of both methane and carbon dioxide are modified by methane oxidation in Zone A. $\delta^{13}\text{C}_{\text{CH}_4}$ is shifted towards high values in a methane-poor environment, as $^{12}\text{CH}_4$ is preferentially oxidised. $\delta^{13}\text{C}_{\text{CO}_2}$ decreased to small values, when the light $^{12}\text{CO}_2$ derived from methane oxidation is added to a small pool of carbon dioxide, in a methane-rich environment (Table 3; Figure 10). However, methane oxidation probably does not entirely explain the large variations of isotopic compositions observed in Zone A (Figures 6 and 7). Station 2E-8, sampled within tailings a few hundred metres away from the wood wastes (Figure 1), does not show any methane in its pore space. Nevertheless, $\delta^{13}\text{C}_{\text{CO}_2}$ increases downward at a rate of 7.5‰/m in Zone A, that is, with a gradient comparable to those observed in profiles acquired within the organic cover (Table 3). Some kind of fractionation process is involved with the dissolved and/or solid phases, but these relations with non-organic phases are beyond the scope of the present research.

Comparison of average $\delta^{13}\text{C}_{\text{CO}_2}$ and $\delta^{13}\text{C}_{\text{CH}_4}$ values measured in Zone B with the type and age of the wood waste fails to outline any strong correlation (Table 3; Figure 11). Average values of $\delta^{13}\text{C}_{\text{CO}_2}$ vary within 10‰, and only a crude tendency to find isotopically heavy CO_2 in older wood wastes is noted. $\delta^{13}\text{C}_{\text{CH}_4}$ vary within 35‰, without any systematic tendency. However, the heavier values are found in Stations 0-8 and C13, where methane has undergone an extensive oxidation. This process shifts the $\delta^{13}\text{C}_{\text{CH}_4}$ to heavier values (Table 3; Figure 10). Omitting these two stations, $\delta^{13}\text{C}_{\text{CH}_4}$ average values range within 10‰.

Figure 13. Simplified model of the carbon cycle in the organic cover.



4.5 SPECIAL CASE: STATION C12

Station C12 shows concentration ratios of methane and carbon dioxide in proportions quite similar to the other stations. Concentration ratios also increase downward for Station C12 as in other stations (Figure 5). However, the $\delta^{13}\text{C}_{\text{CH}_4}$ trend for Station C12 is opposite to those observed at all other stations included in this study (Figure 7). Moreover, it is the sole station for which the data falls near the field of methanogenesis by CO_2 reduction (Figure 10).

The usual $\delta^{13}\text{C}_{\text{CH}_4}$ trend at East Sullivan is a downward decrease of isotopic values (Figure 7). Hornibrook *et al.* (1997) found similar trends in vertical profiles of dissolved gases sampled in wetlands. They noted that the isotopic composition of dissolved CO_2 and CH_4 was pointing to a shift from fermentation to CO_2 reduction with increased depth. They explained that trend by the greater availability of labile, reactive, substrates at the top of the profiles as a result of primary productivity. Methanogenesis shifted to CO_2 reduction in the underlying peat, devoid of reactive material besides downward migrating substrates.

At East Sullivan, detailed examination of isotopic results with respect to sample depth has shown that the heavy $\delta^{13}\text{C}_{\text{CH}_4}$ near surface are the result of methane oxidation (Section 4.3; Figures 10 and 11). The “normal” trend at East Sullivan is not related, in any way, to a change in the dominant methanogenesis pathway. However, the C12 trend is inverse and related to such a change. Light $\delta^{13}\text{C}_{\text{CH}_4}$ at shallow depth plot in Whiticar's *et al.* (1986) CO_2 reduction field, whereas heavy $\delta^{13}\text{C}_{\text{CH}_4}$ at the bottom of the profile is related to fermentation (Figure 11; Appendix B5).

C12 features the younger wood wastes sampled at East Sullivan. Since the methanogenesis pathway is related to substrate reactivity, it is concluded that methane is first produced by CO₂ reduction, given the refractory character of wood fibers. Nevertheless, degradation does occur in aerobic and anaerobic zones, which allows downward migration of more labile substrates, with time. The methanogenesis pathway thus changes to fermentation, which is the main pathway observed elsewhere, at East Sullivan.

CONCLUSION AND RECOMMENDATIONS

The primary goal of this study was to investigate the effects of on-going biodegradational processes on the composition of pore gases in the organic cover of the East Sullivan site. It was hoped that the dominant production pathways for bio-gases would be identified and that this information could lead to a better understanding of the carbon cycle within that cover. This information is required in order to establish a time frame for which the organic cover would prove to be efficient as a response to the problems of Acid Mine Drainage.

Although we were unable to provide an exact period within which the organic cover will remain efficient in its present capacity, the majority of this project's goal was successfully fulfilled. Through the use of isotopic results, concentration ratios and enrichment/depletion trends, two distinct zones have been identified. Zone A is located between the surface of the organic cover and depths of 0.5 to 0.7 metres. This zone is an open system in which atmospheric oxygen readily diffuses and is consumed by carbon oxidation. Methane also undergoes oxidation in that zone, as reflected by the altered isotope ratios of coexisting methane and carbon dioxide, compared to those sampled below that zone. Zone B is located between Zone A and the water table. Anaerobic conditions prevail and biogenic methane production is present. Lack of significant enrichment or depletion in the isotope trends are testimony to the fact that this zone is a partially closed system in which biogenic gases may leave but atmospheric gases are not able to penetrate.

$\delta^{13}\text{C}_{\text{CO}_2}$ and $\delta^{13}\text{C}_{\text{CH}_4}$ data have demonstrated that the apparent dominant production pathway of biogenic methane is fermentation. Although it is not possible to accurately indicate the exact proportion by which fermentation dominates over CO_2 reduction, it is likely that the overall system at East Sullivan is still in a young state, where

the source of available organic matter is large. The youngest station sampled, C12, is exceptional in that methane produced by CO₂ reduction is observed in the upper part of the profile. Commonly, CO₂ reduction characterises old, poorly reactive organic substrates. CO₂ reduction in these recent wood wastes is best explained by the refractory nature of forest residues, which require at least several months of decomposition in order to produce reactive material that can sustain fermentation.

Methane is generally more abundant, and CO₂ carbon isotopes somewhat heavier in the older wood wastes. Besides this, all isotopic results are similar, regardless of the age and type of wood wastes or the presence/absence of raw sewage on the organic cover. We are therefore able to conclude that the organic cover at the East Sullivan site will most likely remain a viable solution to the problems of Acid Mine Drainage well into the next century.

Several recommendations can be made concerning the pursuit of this project. First of all, it would be of interest to repeat sampling and analysis after an appropriate delay of at least five years, in order to acquire information concerning the evolution of the system and its efficiency over time. Secondly, it would be of interest to expand sampling to stations in other areas of the organic cover and at greater depths, in order to improve the three dimensional view of the biogenic system at work. Thirdly, a similar study should be completed on an older organic deposit, in order to evaluate the time period within which fermentation can prevail and the organic cover at East Sullivan will remain efficient. Finally, it would be of interest to include δD determinations in future investigations, in order to allow for a more precise evaluation of the biogenic production pathways through which methane is created.

REFERENCES

Blowes, D.W., Ptacek, C.J., Jambor, J.L. 1994. Remediation and prevention of low-quality drainage from tailings impoundments. *In*: Jambor, J.L. and Blowes, D.W. (eds), *Environmental geochemistry of sulfide mine-wastes*. Mineralogical Association of Canada, Short Course Handbook vol. 22, 365-379.

Centre de recherches industrielles du Québec (CRIQ). 1991. Barrière humide et combustion spontanée. Rapport présenté au service des projets de développement technologique du Centre de recherche minérales, Ministère des Ressources naturelles; 4 pages.

Coleman, D.D., Risatti, B.J., Schoell, M. 1981. Fractionation of carbon and hydrogen isotopes by methane-oxidizing bacteria. *Geochimica et Cosmochimica Acta*, vol. 45, 1033-1037.

Collin, M. 1987. Mathematical modelling of water and oxygen transport in layered soil covers for deposits of pyritic mine tailings. Licentiate treatise, Royal Institute of Technology. Stockholm, Sweden.

Craig, H. 1957. Isotopic standards for carbon and oxygen and correction factors for mass spectrometric analysis of carbon dioxide. *Geochimica et Cosmochimica Acta*, vol. 12, 133-149.

Environment Canada. 1991. The State of Canada's Environment. D.W. Friesen and Sons Limited. Altona, Manitoba, 987 pages.

Froelich, P.N.; Kinkhammer, G.P.; Bender, M.L.; Luedtke, N.A.; Heath, G.R.; Cullen, D.; Dauphin, P.; Hammond, D.; Hartman, B.; Maynard, V. 1979. Early oxidation of organic matter in pelagic sediments of the Eastern Equatorial Atlantic: suboxic diagenesis. *Geochim. Cosmochim. Acta*, vol. 43, 1075-1090.

Germain, M.D., Tassé, N., Bergeron, M. 1992. Efficacité des copeaux de bois comme couverture pour les résidus miniers. Rapport présenté au Centre de recherche minérales, MERQ; 22 pages.

Happell, J.D., Chanton, J.P., Showers, W.S., 1994. The influence of methane oxidation on the stable isotopic composition of methane emitted from Florida swamp forests. *Geochimica et Cosmochimica Acta*, vol. 58, 4377-4388.

Hornibrook, E.R.C., Longstaffe, F.J., Fyfe, W.S., 1997. Spatial distribution of microbial methane production pathways in temperate zone wetland soils: stable carbon and hydrogen isotope evidence. *Geochimica et Cosmochimica Acta*, vol. 61, 745-753.

Jenden, P.D., Kaplan, I.R. 1986. Comparison of microbial gases from the Middle America Trench and Scripps Submarine Canyon: Implications for the origin of natural gas. *Applied Geochemistry*, vol. 1, 631-646.

Karam, A., Azzaria, L.M. 1990. Étude en laboratoire portant sur la restauration du parc à résidus de l'ancienne mine East-Sullivan. 98 pages.

Martens, C.S., Blair, N.E., Green, C.D., Des Marais, D.J. 1986. Seasonal variations in the stable carbon isotopic signature of biogenic methane in a coastal sediment. *Science*, vol. 223, 1300-1303.

Merritt, D.A., Hayes, J.M., Des Marais, D.J., 1995. Carbon isotopic analysis of atmospheric methane by isotope-ratio-monitoring gas chromatography-mass spectrometry. *Journal of Geophysical Research*, vol. 100, 1317-1326.

Paine, P.J. 1987. An historic and geographic overview of acid mine drainage. *In: Comptes rendus du séminaires/atelier sur le drainage minier acide, 23-23 mars, 1987.* Halifax, Nouvelle Ecosse. Conservation et Protection, Environnement Canada et Groupe de gestion des aéroports, transport Canada, Ottawa, Ontario.

Paquet, A. 1992. La conception d'une barrière humide a l'aide de résidus forestiers. Ministère de l'Energie et des Ressources; 24 pages.

Pine, M.J., Barker, H.A. 1956. Studies on methane fermentation XII. The pathway of hydrogen in the acetate fermentation. *Journal of Bacteriology*, vol. 71, 644-648.

Planigram. 1987. Étude de caractérisation du parc à résidus minier East-Sullivan, pour les ministères de l'Énergie et des Ressources et de l'Environnement du Québec.

Reardon, E.J., Moddle, P.M. 1985. Suitability of peat as an oxygen interceptor material for the close-out of pyritic uranium tailings: column studies. *Uranium*, vol. 2, 83-110.

Reardon, E.J., Poscente, P.J. 1984. A study of gas compositions in sawmill waste deposits: Evaluation of the use of wood waste in close-out of pyritic tailings. *Reclamation and Revegetation Research*, vol. 3, 109-128.

Roche Ltée, Groupe-conseil. 1994. Parcelles expérimentales au parc East-Sullivan - rapport d'étape 1994 et rapport final. Centre de recherches minérales, Ministère de l'Énergie et des Ressources du Québec, 19 pages et 2 annexes.

Schoell, M. 1980. The hydrogen and carbon isotopic composition of methane from natural gases of various origins. *Geochimica et Cosmochimica Acta*, vol. 44, 649-661.

Schoell, M. 1988. Multiple origins of methane in the earth. *Chemical Geology*, vol. 71, 1-10.

Sherwood Lollar, B. Frape, S.K., Weise, S.M. 1994. New Sampling devices for environmental characterization of groundwater and dissolved gas chemistry (CH₄, N₂, He). *Environmental Science Technology*, vol. 28, 2423-2427.

Tassé, N., Germain, M.D., Bergeron, M. 1994. Composition of interstitial gases in wood chips deposited on reactive mine tailings; consequences for their use as an oxygen barrier. *In* : Blowes, D.W. and Alpers, C.N. (eds) *The Environmental Geochemistry of Sulfide Oxidation*. American Chemical Society, Symposium Series 550, 631-644.

Tassé, N., Germain, M.D. 1996. Qualité des eaux résiduelles au site East Sullivan: Rapport final présenté au service du développement minier, Ministère des ressources naturelle du Québec; 251 pages.

Tassé, N., Germain, M.D., Dufour, D., Tremblay, R. 1997. Organic-Waste Cover over the East Sullivan Mine Tailings: Beyond the Oxygen Barrier. Fourth International Conference on Acid Rock Drainage. Vancouver, B.C. May 31- June 6, 1998. Pages 1627-1642.

Université de Sherbrooke, Département de génie civil. 1988. Projet de restauration du parc à résidus de la mine East Sullivan par l'utilisation de résidus organiques. 110 pages.

Whiticar, M.J., Faber, E., Schoell, M. 1986. Biogenic methane formation in marine and freshwater environments: CO₂ reduction vs. acetate fermentation - isotope evidence. *Geochimica et Cosmochimica Acta*, vol. 50, 693-709.

Woltemate, I., Whiticar, M.J., Schoell, M., 1984. Carbon and hydrogen isotopic composition of bacterial methane in a shallow freshwater lake. *Limnology and Oceanology*, vol. 29, 985-992.

Appendix A

Laboratory Tests & Analytical Verifications

Site Photographs

Table A-1. Outline of procedure used to obtain the best possible separation of the ion-current peaks.

Parameter Changed	Trial Number	Oven Temperature (°C)	Injection Temperature (°C)	Detector Temperature (°C)	Flow Rate (ml/min)	Column Head Pressure (psi)	Results
Start	0	Room (25-28)	200	200	30	12	Ion current peaks separated but very close
Oven	1	50	200	200	30	12	Ion current peaks closer
Oven	2	100	200	200	30	12	Ion current peaks almost fused
Verification	3	Room (25-28)	200	200	30	12	Same as Trial 0
Injector	4	Room (25-28)	175	200	30	12	Less separation than trial 3
Injector	5	Room (25-28)	225	200	30	12	Better separation than trial 3 & 4
Injector	6	Room (25-28)	240	200	30	12	Better separation than trial 5
Injector	7	Room (25-28)	250	200	30	12	Better separation than trial 6
Verification	8	Room (25-28)	250	200	30	12	Same as Trial 7
Detector	9	Room (25-28)	250	175	30	12	Less separation than trial 8
Detector	10	Room (25-28)	250	225	30	12	Better separation than trials 8 & 9
Detector	11	Room (25-28)	250	250	30	12	Better separation than trial 10
Verification	12	Room (25-28)	250	200	30	12	Same as Trial 7
Flow Rate	13	Room (25-28)	250	250	35	12	Less separation than trial 11
Flow Rate	14	Room (25-28)	250	250	40	12	Better separation than trial 13
Flow Rate	15	Room (25-28)	250	250	25	12	Better separation than trials 11 through 14
Flow Rate	16	Room (25-28)	250	250	20	12	Better separation than trials 11 through 15
Flow Rate	17	Room (25-28)	250	250	15	12	Less separation than trial 16
Verification	18	Room (25-28)	250	250	30	12	Same as Trial 11
C.H. Pressure**	19	Room (25-28)	250	250	20	13	Less separation than trial 17
C.H. Pressure**	20	Room (25-28)	250	250	20	14	Less separation than trials 17 & 19
C.H. Pressure**	21	Room (25-28)	250	250	20	11	Better separation than trial 20
C.H. Pressure**	22	Room (25-28)	250	250	20	10	Better separation than trial 21
C.H. Pressure**	23	Room (25-28)	250	250	20	9	Less separation than trial 22
Verification	24	Room (25-28)	250	250	20	10	Same as Trail 22

Best Separation Possible

Verification	22 & 24	Room (25-28)	250	250	20	10	Same as Trail 22 & 24
--------------	---------	--------------	-----	-----	----	----	-----------------------

*Altered parameter is located in shaded area.

** C.H. Pressure = Column Head Pressure

Table A-2. Analytical Conditions and Isotopic Results from Laboratory Test A.

Laboratory Test A	
Combustion Furnace = 850 C	
Sample Composition = 9.98% Methane & 90.02% Argon	
Injection Amount = 40 microlitres (All from Vial #11)	
Sample #	Carbon Isotope Ratio (per mil)
1	-18.4
2	-18.8
3	-19.1
4	-19.1
5	-18.8
6	-18.6
7	-18.5
8	-19.2
9	-17.8
10	-18.8
Average	-18.7
Standard Deviation	0.4

*Carbon isotope ratios are expressed as per mil and are relative to PDB.

Table A-3. Analytical Conditions and Isotopic Results from Laboratory Test B.

Laboratory Test B	
Combustion Furnace = 900 C	
Sample Composition = 9.98% Methane & 90.02% Argon	
Injection Amount = 40 microlitres (All from Vial #12)	
Sample #	Carbon Isotope Ratio (per mil)
1	-17.7
2	-17.1
3	-17.4
4	-17.6
5	-17.5
6	-17.3
7	-18.0
8	-17.6
9	-17.6
10	-17.8
Average	-17.5
Standard Deviation	0.3

*Carbon isotope ratios are expressed as per mil and are relative to PDB.

Table A-4. Analytical Conditions and Isotopic Results from Laboratory Test C.

Laboratory Test C		
Combustion Furnace = 850 C		
Sample Composition = 5% Methane, 5% Carbon Dioxide & 90% Helium		
Injection Amount = 40 microlitres (All from Vial #13)		
Sample #	Carbon Isotope Ratio for Methane (per mil)	Carbon Isotope Ratio for Carbon Dioxide (per mil)
1	-33.8	-39.4
2	-34.3	-39.1
3	-34.0	-39.3
4	-34.6	-38.8
5	-33.8	-39.2
6	-34.7	-39.4
7	-33.9	-39.3
8	-33.8	-39.5
9	-33.7	-39.0
10	-34.6	-39.4
Average	-34.1	-39.2
Standard Deviation	0.4	0.2

*Carbon isotope ratios are expressed as per mil and are relative to PDB.

Table A-5. Analytical Conditions and Isotopic Results from Laboratory Test D.

Laboratory Test D		
Combustion Furnace = 900 C		
Sample Composition = 5% Methane, 5% Carbon Dioxide & 90% Helium		
Injection Amount = 40 microlitres (All from Vial #14)		
Sample #	Carbon Isotope Ratio for Methane (per mil)	Carbon Isotope Ratio for Carbon Dioxide (per mil)
1	-34.3	-39.3
2	-34.3	-39.3
3	-34.5	-39.1
4	-34.4	-38.9
5	-33.9	-39.3
6	-34.6	-39.2
7	-34.1	-39.0
8	-34.4	-39.3
9	-34.0	-39.5
10	-33.8	-39.1
Average	-34.3	-39.2
Standard Deviation	0.3	0.2

*Carbon isotope ratios are expressed as per mil and are relative to PDB.

Table A-6. System Stability Values for the Analytical System.

Date	Time	Average Value of Stability Run (Ratio 2/1)
January	--	--
29	12:41	2.6557E-07
29	15:41	3.1584E-07
30	9:26	4.0540E-07
30	15:48	2.8549E-07
February	--	--
3	9:49	1.5039E-07
3	15:12	2.1345E-07
3	21:20	4.4224E-07
4	9:23	2.5482E-07
4	14:33	4.3727E-07
4	18:35	2.7519E-07
5	9:15	4.6032E-07
5	16:59	4.3117E-07
6	9:06	3.7899E-07
6	14:59	3.4623E-07
6	20:56	3.4713E-07
7	9:33	1.4627E-07
7	16:15	2.8780E-07
7	23:06	4.2897E-07
9	10:28	4.2244E-07
9	19:59	2.1695E-07
10	8:55	2.5792E-07
10	15:51	3.3404E-07
11	9:12	2.1547E-07
11	14:36	4.7134E-07
12	12:25	2.4678E-07
12	16:03	2.9216E-07
14	9:03	2.5471E-07
14	10:58	2.0793E-07
14	11:09	3.0259E-07
14	11:55	4.3175E-07
Average =		3.1755E-07

Table A-7. Analytical Conditions and Isotopic Results from Laboratory Test E.

Laboratory Test E		
Combustion Furnace = 900 C		
Sample Composition = 5% Methane, 5% Carbon Dioxide, 45% Argon & 45% Helium		
Injection Amount = 25 microlitres		
Vial #	Carbon Isotope Ratio for Methane (per mil)	Carbon Isotope Ratio for Carbon Dioxide (per mil)
15	-18.1	-17.8
16	-18.7	-17.5
17	-18.6	-17.2
18	-18.1	-17.6
19	-18.2	-17.5
20	-18.5	-17.6
21	-18.8	-17.1
Average	-18.4	-17.5
Standard Deviation	0.3	0.2

*Carbon isotope ratios are expressed as per mil and are relative to PDB.

Table A-8. Analytical Conditions and Isotopic Results from Laboratory Test F.

Laboratory Test F	
Combustion Furnace = 900 C	
Sample Composition = 50% Methane & 50% Helium	
Injection Amount = 5 microlitres (All from Vial #22)	
Trial # (Same Vial)	Carbon Isotope Ratio for Methane (per mil)
1	-33.2
2	-33.6
3	-33.7
4	-33.6
5	-33.2
6	-33.6
7	-33.3
8	-33.1
9	-34.2
10	-33.6
Average	-33.5
Standard Deviation	0.3

*Carbon isotope ratios are expressed as per mil and are relative to PDB.

Table A-9. Analytical precision verifications

Day 1: February 3, 1997

Before Sample Analyses		
Trial Vial Analysed (#)	Verification Number	Carbon Isotope Ratio (per mil)
1	1	-17.4
1	2	-17.4
1	3	-17.6
1	4	-17.1
1	5	-17.2
Average		-17.3
Standard Deviation		0.2

During Sample Analyses		
Trial Vial Analysed (#)	Verification Number	Carbon Isotope Ratio (per mil)
1	1	-17.5
1	2	-17.4
1	3	-
1	4	-
1	5	-
Average		-17.5
Standard Deviation		0.1

After Sample Analyses		
Trial Vial Analysed (#)	Verification Number	Carbon Isotope Ratio (per mil)
1	1	-17.2
1	2	-17.9
1	3	-18.0
1	4	-17.5
1	5	-17.6
Average		-17.6
Standard Deviation		0.3

Day 2: February 4, 1997

Before Sample Analyses		
Trial Vial Analysed (#)	Verification Number	Carbon Isotope Ratio (per mil)
2	1	-18.4
2	2	-18.5
2	3	-18.2
2	4	-18.2
2	5	-18.5
Average		-18.4
Standard Deviation		0.2

During Sample Analyses		
Trial Vial Analysed (#)	Verification Number	Carbon Isotope Ratio (per mil)
2	1	-18.3
2	2	-
2	3	-
2	4	-
2	5	-
Average		-18.3
Standard Deviation		-

After Sample Analyses		
Trial Vial Analysed (#)	Verification Number	Carbon Isotope Ratio (per mil)
2	1	-18.8
2	2	-18.4
2	3	-18.5
2	4	-18.2
2	5	-
Average		-18.5
Standard Deviation		0.2

Day 3: February 5, 1997

Before Sample Analyses		
Trial Vial Analysed (#)	Verification Number	Carbon Isotope Ratio (per mil)
3	1	-17.8
3	2	-17.5
3	3	-17.9
3	4	-17.9
3	5	-17.2
Average		-17.7
Standard Deviation		0.3

During Sample Analyses		
Trial Vial Analysed (#)	Verification Number	Carbon Isotope Ratio (per mil)
3	1	-17.9
3	2	-17.6
3	3	-
3	4	-
3	5	-
Average		-17.7
Standard Deviation		0.2

After Sample Analyses		
Trial Vial Analysed (#)	Verification Number	Carbon Isotope Ratio (per mil)
3	1	-17.8
3	2	-17.6
3	3	-17.3
3	4	-17.1
3	5	-17.5
Average		-17.5
Standard Deviation		0.3

*Combustion Furnace = 900 °C

**Sample Composition = 5% methane, 5% carbon dioxide, 45% argon and 45% helium.

***Injection Amount (all samples) = 40 microlitres

Table A-9 (continued). Analytical precision verifications

Day 4: February 6, 1997

Before Sample Analyses		
Trial Vial Analysed (#)	Verification Number	Carbon Isotope Ratio (per mil)
4	1	-18.0
4	2	-17.9
4	3	-17.8
4	4	-18.3
4	5	-17.6
Average		-17.9
Standard Deviation		0.3

During Sample Analyses		
Trial Vial Analysed (#)	Verification Number	Carbon Isotope Ratio (per mil)
4	1	-17.6
4	2	-17.8
4	3	--
4	4	--
4	5	--
Average		-17.7
Standard Deviation		0.1

After Sample Analyses		
Trial Vial Analysed (#)	Verification Number	Carbon Isotope Ratio (per mil)
4	1	-18.4
4	2	-18.1
4	3	-17.9
4	4	-18.3
4	5	--
Average		-18.2
Standard Deviation		0.2

Day 5: February 7, 1997

Before Sample Analyses		
Trial Vial Analysed (#)	Verification Number	Carbon Isotope Ratio (per mil)
5	1	-18.2
5	2	-18.3
5	3	-18.3
5	4	--
5	5	--
Average		-18.3
Standard Deviation		0.1

During Sample Analyses		
Trial Vial Analysed (#)	Verification Number	Carbon Isotope Ratio (per mil)
5	1	-18.0
5	2	-17.9
5	3	--
5	4	--
5	5	--
Average		-18.0
Standard Deviation		0.1

After Sample Analyses		
Trial Vial Analysed (#)	Verification Number	Carbon Isotope Ratio (per mil)
5	1	-18.4
5	2	-18.3
5	3	-18.3
5	4	--
5	5	--
Average		-18.3
Standard Deviation		0.1

Day 6: February 9, 1997

Before Sample Analyses		
Trial Vial Analysed (#)	Verification Number	Carbon Isotope Ratio (per mil)
6	1	-17.6
6	2	-17.9
6	3	-18.2
6	4	--
6	5	--
Average		-17.9
Standard Deviation		0.3

During Sample Analyses		
Trial Vial Analysed (#)	Verification Number	Carbon Isotope Ratio (per mil)
6	1	-17.5
6	2	--
6	3	--
6	4	--
6	5	--
Average		-17.5
Standard Deviation		--

After Sample Analyses		
Trial Vial Analysed (#)	Verification Number	Carbon Isotope Ratio (per mil)
6	1	-17.9
6	2	-17.8
6	3	-17.3
6	4	--
6	5	--
Average		-17.7
Standard Deviation		0.3

*Combustion Furnace = 900 °C

**Sample Composition = 5% methane, 5% carbon dioxide, 45% argon and 45% helium.

***Injection Amount (all samples) = 40 microlitres

Table A-9 (continued). Analytical precision verifications

Day 7: February 10, 1997

Before Sample Analyses		
Trial Vial Analysed (#)	Verification Number	Carbon Isotope Ratio (per mil)
7	1	-18.0
7	2	-18.7
7	3	-18.5
7	4	--
7	5	--
Average		-18.4
Standard Deviation		0.3

During Sample Analyses		
Trial Vial Analysed (#)	Verification Number	Carbon Isotope Ratio (per mil)
7	1	-18.5
7	2	-18.0
7	3	--
7	4	--
7	5	--
Average		-18.3
Standard Deviation		0.3

After Sample Analyses		
Trial Vial Analysed (#)	Verification Number	Carbon Isotope Ratio (per mil)
7	1	-18.2
7	2	-18.6
7	3	-18.2
7	4	-18.7
7	5	-18.8
Average		-18.5
Standard Deviation		0.3

Day 8: February 11, 1997

Before Sample Analyses		
Trial Vial Analysed (#)	Verification Number	Carbon Isotope Ratio (per mil)
8	1	-18.1
8	2	-18.2
8	3	-18.0
8	4	-18.2
8	5	-18.2
Average		-18.2
Standard Deviation		0.1

During Sample Analyses		
Trial Vial Analysed (#)	Verification Number	Carbon Isotope Ratio (per mil)
8	1	-18.4
8	2	-18.2
8	3	--
8	4	--
8	5	--
Average		-18.3
Standard Deviation		--

After Sample Analyses		
Trial Vial Analysed (#)	Verification Number	Carbon Isotope Ratio (per mil)
8	1	-18.3
8	2	-18.4
8	3	-18.3
8	4	-18.3
8	5	-18.5
Average		-18.3
Standard Deviation		0.1

Day 9: February 12, 1997

Before Sample Analyses		
Trial Vial Analysed (#)	Verification Number	Carbon Isotope Ratio (per mil)
9	1	-17.5
9	2	-17.0
9	3	-17.2
9	4	-16.8
9	5	-16.9
Average		-17.1
Standard Deviation		0.3

During Sample Analyses		
Trial Vial Analysed (#)	Verification Number	Carbon Isotope Ratio (per mil)
9	1	-17.1
9	2	-17.5
9	3	-17.5
9	4	--
9	5	--
Average		-17.4
Standard Deviation		0.2

After Sample Analyses		
Trial Vial Analysed (#)	Verification Number	Carbon Isotope Ratio (per mil)
9	1	-16.8
9	2	-17.2
9	3	-17.4
9	4	-16.9
9	5	--
Average		-17.1
Standard Deviation		0.3

*Combustion Furnace = 900 °C

**Sample Composition = 5% methane, 5% carbon dioxide, 45% argon and 45% helium.

***Injection Amount (all samples) = 40 microlitres

Table A-9 (continued). Analytical precision verifications

Day 10: February 14, 1997

Before Sample Analyses		
Trial Vial Analysed (#)	Verification Number	Carbon Isotope Ratio (per mil)
10	1	-19.1
10	2	-18.6
10	3	-18.6
10	4	--
10	5	--
Average		-18.8
Standard Deviation		0.3

During Sample Analyses		
Trial Vial Analysed (#)	Verification Number	Carbon Isotope Ratio (per mil)
10	1	-18.5
10	2	--
10	3	--
10	4	--
10	5	--
Average		-18.5
Standard Deviation		--

After Sample Analyses		
Trial Vial Analysed (#)	Verification Number	Carbon Isotope Ratio (per mil)
10	1	-18.9
10	2	-19.3
10	3	--
10	4	--
10	5	--
Average		-19.1
Standard Deviation		0.2

*Combustion Furnace = 900 °C

**Sample Composition = 5% methane, 5% carbon dioxide, 45% argon and 45% helium.

***Injection Amount (all samples) = 40 microlitres





Photo 1: Mine Tailings impoundment with a retention dike in the foreground and the limit of the organic cover in the distance (October, 1996).



Photo 2: Photo taken from the top of the organic cover showing the mine tailings with the inner edge of the organic cover in the distance (October, 1996).



Photo 3: Photo taken on top of the mine tailings impoundment in an area where no organic cover is present (October, 1996).



Photo 4: Photo taken from the top of the organic cover showing the mine tailings with the inner edge of the organic cover (October, 1996).

Appendix B

Isotopic Results

Table B-1. Isotopic Results from Station C1.

Station C1						
Depth (cm)	$\delta^{13}\text{C} - \text{CO}_2$ (‰)	$\delta^{13}\text{C} - \text{CH}_4$ (‰)	System Stability (Ratio 2/1)	Peak Area CO_2	Peak Area CH_4	Peak Area Ratio $(\text{CH}_4/\text{CO}_2) \times 100$
10		-54.2	2.03E-07		1.3E-09	
10	-19.8	-53.8	4.01E-07	4.1E-09	1.0E-08	243.9
20	-20.0	-49.5	1.82E-07	1.7E-08	4.9E-08	288.2
30	-20.7	-55.3	4.07E-07	3.8E-09	8.0E-09	210.5
40						
50	-20.4	-48.1	3.31E-07	1.2E-10	2.6E-10	216.7
60	-21.1	-57.2	1.56E-07	3.8E-09	1.0E-08	263.2
70	-13.5	-53.7	3.52E-07	4.4E-09	1.1E-08	250.0
80	-20.2	-53.0	4.10E-07	4.1E-09	9.5E-09	231.7
90						
100		-49.7	4.86E-08		3.3E-09	
110	-18.6	-55.6	7.94E-08	1.6E-08	6.5E-08	406.3
120						
130	-12.3	-52.8	1.80E-07	3.5E-09	9.3E-09	265.7
Average Value	-18.5	-53.0	2.50E-07	6.3E-09	1.6E-08	254.4

Figure B-1.

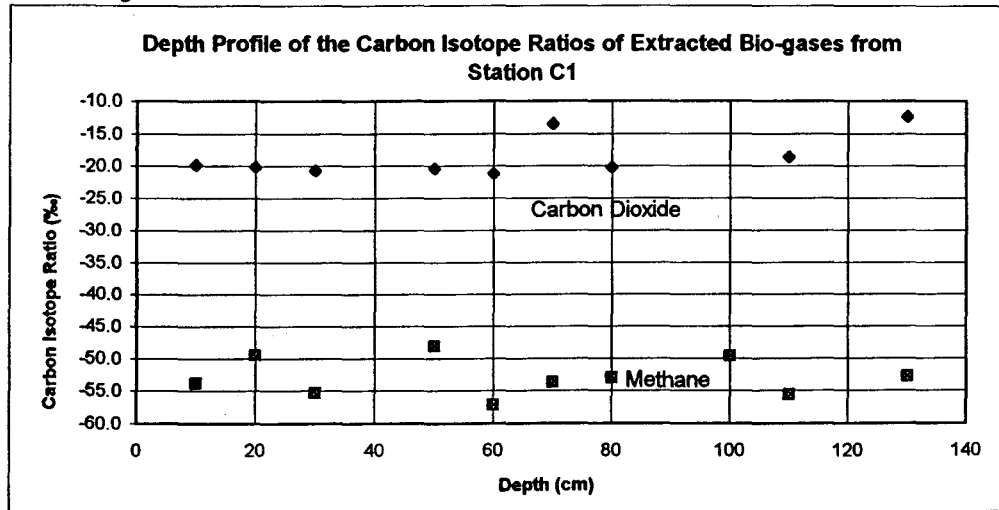


Table B-2. Isotopic Results from Station C4.

Station C4						
Depth (cm)	$\delta^{13}\text{C} - \text{CO}_2$ (‰)	$\delta^{13}\text{C} - \text{CH}_4$ (‰)	System Stability (Ratio 2/1)	Peak Area CO_2	Peak Area CH_4	Peak Area Ratio $(\text{CH}_4/\text{CO}_2) \times 100$
10	-22.0		4.39E-07	9.3E-09		
20	-23.2		9.71E-08	1.2E-08		
20	-22.8		1.53E-08	1.3E-08		
30	-16.6		2.85E-07	1.3E-09		
40	-18.8	-45.1	1.23E-07	4.8E-09	1.8E-09	37.5
50	-20.4	-47.0	1.01E-07	2.2E-08	6.4E-09	29.1
60	-20.1	-46.8	3.29E-07	5.8E-09	1.8E-09	31.0
70	-16.2	-50.1	1.69E-07	2.7E-09	1.7E-09	63.0
80	-16.6	-51.6	1.78E-07	3.1E-09	1.9E-09	61.3
90	-14.4	-50.2	1.86E-07	3.0E-09	1.5E-09	50.0
100	-15.6	-53.6	1.72E-07	1.6E-09	1.1E-09	68.8
110	-15.3	-50.8	1.90E-07	5.6E-09	2.8E-09	50.0
110	-15.6	-51.7	3.48E-07	3.6E-09	1.9E-09	52.8
120	-14.4	-49.6	3.49E-07	2.6E-09	2.2E-09	84.6
130	-15.4	-53.3	5.49E-07	2.5E-09	1.9E-09	76.0
140	-14.0	-49.5	1.93E-07	2.7E-09	2.4E-09	88.9
150	-14.6	-50.9	1.92E-07	2.8E-09	2.4E-09	85.7
Average Value	-17.4	-50.0	2.30E-07	5.8E-09	2.3E-09	59.9

Figure B-2.

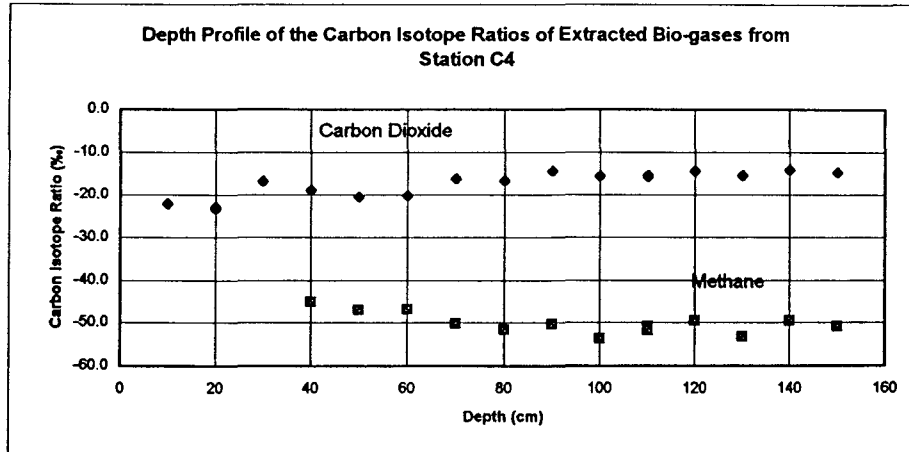


Table B-3. Isotopic Results from Station C6.

Station C6						
Depth (cm)	$\delta^{13}\text{C} - \text{CO}_2$ (‰)	$\delta^{13}\text{C} - \text{CH}_4$ (‰)	System Stability (Ratio 2/1)	Peak Area CO_2	Peak Area CH_4	Peak Area Ratio $(\text{CH}_4/\text{CO}_2)*100$
10	-18.9	-30.0	1.83E-07	8.6E-09	1.4E-09	16.3
20	-21.4	-32.7	2.21E-07	8.6E-09	1.8E-09	20.9
30	-21.3	-43.4	1.39E-07	1.1E-08	2.4E-09	21.8
40						
50	-21.3	-50.0	1.64E-07	8.9E-09	2.2E-09	24.7
60	-22.0	-50.9	2.91E-07	1.7E-08	3.6E-09	21.2
70	-18.0	-53.6	2.33E-07	2.0E-08	4.1E-09	20.5
80	-19.6	-52.4	2.18E-07	1.7E-08	3.5E-09	20.6
80	-19.7	-52.3	1.88E-07	1.6E-08	3.4E-09	21.3
90	-17.2		5.95E-08	1.8E-08		
90	-17.7		6.36E-08	1.7E-08		
100	-19.1		1.22E-07	1.7E-08		
110	-19.0		3.44E-07	1.9E-08		
120	-18.5		1.97E-07	1.9E-08		
130	-19.3		2.36E-07	3.3E-09		
140	-18.1		2.29E-07	3.4E-09		
140	-18.1		2.83E-07	1.4E-08		
140	-18.8		3.38E-07	1.9E-08		
150	-16.9		3.26E-07	1.9E-08		
150	-17.7		2.37E-07	2.0E-08		
Average Value	-19.1	-45.7	2.14E-07	1.5E-08		20.9

Figure B-3.

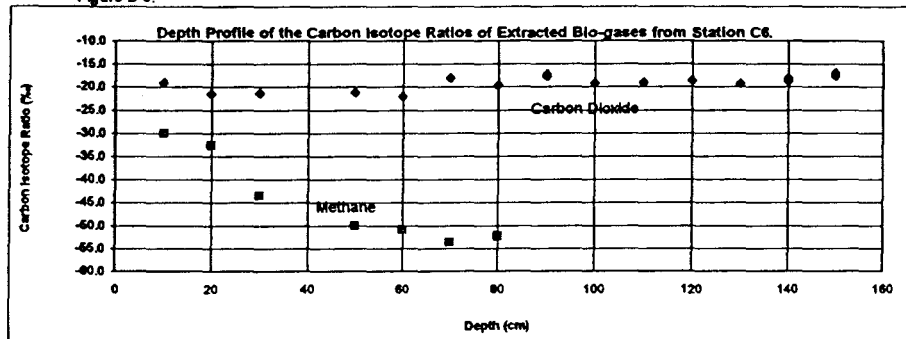


Table B-4. Isotopic Results from Station C7.

Station C7						
Depth (cm)	$\delta^{13}\text{C} - \text{CO}_2$ (‰)	$\delta^{13}\text{C} - \text{CH}_4$ (‰)	System Stability (Ratio 2/1)	Peak Area CO_2	Peak Area CH_4	Peak Area Ratio $(\text{CH}_4/\text{CO}_2) \times 100$
10	-20.6	-31.0	7.94E-08	9.1E-09	1.4E-09	15.4
10	-20.7	-33.6	2.34E-07	4.3E-09	1.3E-09	30.2
20	-18.6	-32.7	2.54E-07	1.0E-08	3.7E-09	37.0
20	-18.9	-34.7	1.29E-07	6.2E-09	1.9E-09	30.6
30	-15.4	-43.4	2.13E-07	7.6E-09	1.6E-08	210.5
30	-15.6	-42.9	9.01E-07	1.3E-08	3.0E-08	230.8
40	-14.7	-46.9	3.67E-07	6.1E-10	1.5E-09	245.9
40	-14.4	-47.4	5.98E-08	1.7E-09	4.2E-09	247.1
50		-50.9	2.96E-07		9.3E-09	
50		-51.0	1.41E-07		4.3E-09	
50	-19.5		2.96E-07	1.4E-09		
60		-50.5	1.44E-07	-	1.4E-08	
60	-15.1	-51.8	2.42E-07	-	2.3E-09	
70	-10.3		2.13E-07	1.1E-09		
70		-53.1	3.99E-07		4.4E-09	
70		-52.5	3.03E-07		2.1E-09	
70		-52.4	1.20E-07		2.4E-09	
80	-10.1	-52.9	2.93E-07	5.0E-10	2.1E-09	420.0
Average Value	-16.2	-45.5	2.60E-07	5.0E-09	6.3E-09	163.1

Figure B-4.

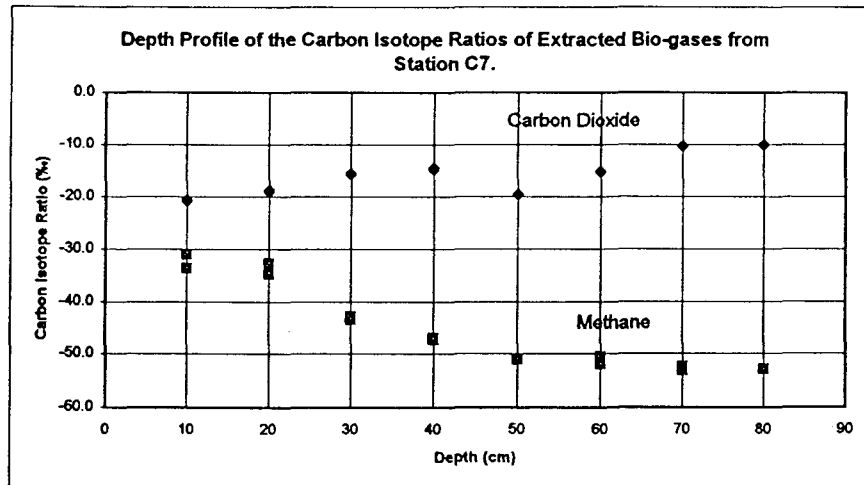


Table B-5. Isotopic Results from Station C12.

Station C12						
Depth (cm)	$\delta^{13}\text{C} - \text{CO}_2$ (‰)	$\delta^{13}\text{C} - \text{CH}_4$ (‰)	System Stability (Ratio 2/1)	Peak Area CO_2	Peak Area CH_4	Peak Area Ratio $(\text{CH}_4/\text{CO}_2) \times 100$
10	-18.5	-69.8	3.12E-07	1.6E-08	1.1E-09	6.9
20	-19.2	-64.2	2.54E-07	1.5E-08	1.0E-09	6.7
30	-18.4	-69.8	5.65E-08	1.6E-08	1.2E-09	7.5
30	-18.9	-74.6	2.33E-07	1.5E-08	1.3E-09	8.7
40	-18.1	-64.2	1.32E-08	1.6E-08	2.2E-09	13.8
50	-18.2	-63.3	2.59E-07	1.7E-08	3.5E-09	20.6
60	-17.3	-59.1	3.69E-07	1.7E-08	3.1E-09	18.2
70	-17.1	-53.8	3.57E-08	1.3E-08	2.5E-09	19.2
70	-16.2	-53.9	2.46E-07	1.4E-08	3.2E-09	22.9
80	-18.0	-53.2	2.91E-07	1.4E-08	3.0E-09	21.4
90	-16.1	-53.0	3.81E-07	1.0E-08	2.7E-09	27.0
100	-17.3	-53.2	1.25E-07	1.6E-08	3.9E-09	24.4
110	-15.5	-51.7	1.77E-07	1.1E-08	2.9E-09	26.4
120	-15.3	-50.6	8.48E-08	1.0E-08	3.0E-09	30.0
Average Value	-17.4	-59.6	2.03E-07	1.4E-08	2.5E-09	18.1

Figure B-5.

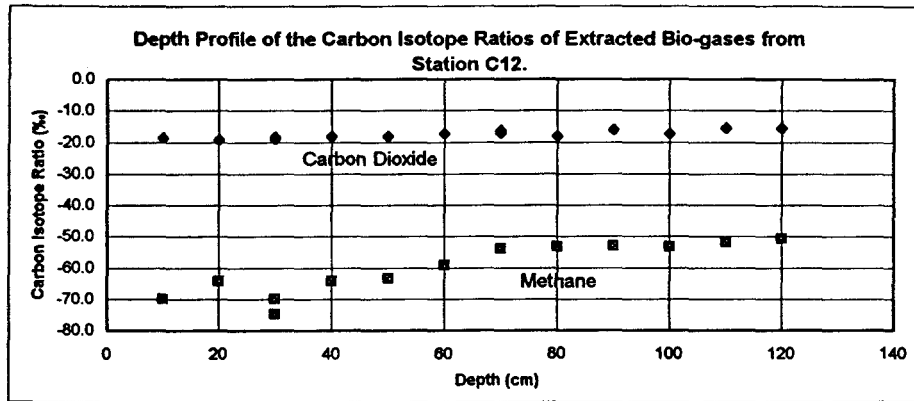


Table B-6. Isotopic Results from Station C13.

Station C13						
Depth (cm)	$\delta^{13}\text{C} - \text{CO}_2$ (‰)	$\delta^{13}\text{C} - \text{CH}_4$ (‰)	System Stability (Ratio 2/1)	Peak Area CO_2	Peak Area CH_4	Peak Area Ratio (CH_4/CO_2)*100
10	-20.1		1.78E-07	1.1E-08		
10	-20.4		3.18E-07	7.6E-09		
20	-19.6		2.26E-07	1.6E-08		
20	-19.3		1.46E-07	3.9E-09		
30	-20.4		2.17E-07	2.1E-08		
40	-18.2	-28.7	1.67E-07	1.4E-08	2.1E-09	15.0
40	-18.2	-25.4	2.63E-08	1.3E-08	2.3E-09	17.7
50						
60	-18.9	-32.3	2.93E-07	1.7E-08	3.6E-09	21.2
60	-17.2	-28.8	2.14E-07	5.8E-09	1.8E-09	31.0
70	-18.3	-30.3	2.87E-07	1.8E-08	3.8E-09	21.1
80	-16.1	-37.9	2.06E-07	1.1E-08	4.2E-09	38.2
80	-15.7	-36.8	3.45E-07	1.1E-08	4.4E-09	40.0
90	-15.8	-34.9	2.55E-07	6.1E-09	2.4E-09	39.3
100	-15.7	-37.0	3.30E-08	7.6E-09	2.4E-09	31.6
110	-15.4	-35.6	1.21E-07	1.1E-08	3.5E-09	31.8
110	-15.8	-34.3	8.60E-07	7.1E-09	2.7E-09	38.0
120	-16.7	-37.4	1.12E-07	6.3E-09	2.7E-09	42.9
130	-16.3	-36.6	1.94E-07	7.7E-09	3.2E-09	41.6
Average Value	-17.7	-33.5	2.33E-07	1.1E-08	3.0E-09	31.5

Figure B-6.

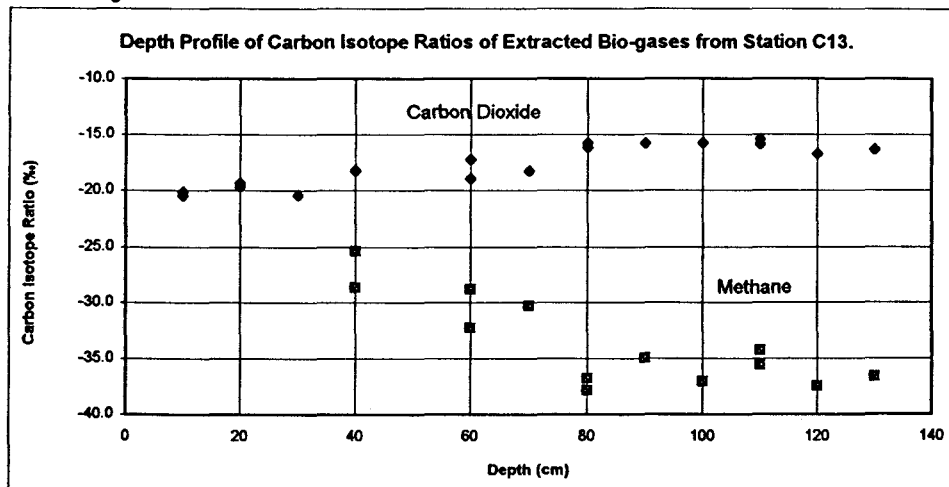


Table B-7. Isotopic Results from Station C14.

Station C14						
Depth (cm)	$\delta^{13}\text{C} - \text{CO}_2$ (‰)	$\delta^{13}\text{C} - \text{CH}_4$ (‰)	System Stability (Ratio 2/1)	Peak Area CO_2	Peak Area CH_4	Peak Area Ratio $(\text{CH}_4/\text{CO}_2)*100$
10	-17.1		2.21E-07	1.4E-08		
20	-18.6		1.13E-07	2.0E-08		
30	-16.7		7.57E-08	2.0E-08		
40	-15.8		1.02E-07	1.7E-08		
50	-16.4		3.77E-07	2.1E-08		
50	-16.2	-43.2	1.09E-07	1.6E-08	8.2E-10	5.1
50	-15.8	-37.5	1.82E-07	2.0E-08	1.1E-09	5.5
60						
70	-16.0	-43.9	2.27E-08	2.7E-08	1.3E-09	4.8
80	-15.8	-50.7	1.05E-07	2.1E-08	1.8E-09	8.6
90	-14.5	-54.7	1.90E-07	2.0E-08	1.2E-09	6.0
90	-14.5	-47.7	6.48E-07	2.7E-08	1.5E-09	5.6
100	-15.8	-41.7	4.88E-08	1.2E-08	1.3E-09	10.8
110	-14.7	-48.3	4.02E-07	1.9E-08	1.1E-09	5.8
110	-14.5	-44.1	2.11E-07	2.0E-08	1.1E-09	5.5
120	-15.9	-30.6	1.44E-07	2.3E-08	8.7E-10	3.8
120	-15.4		2.38E-07	2.2E-08		
120	-16.0		2.27E-07	2.0E-08		
130	-13.5		1.64E-07	3.5E-09		
130	-14.9	-54.5	1.40E-07	1.8E-08	1.4E-09	7.8
140	-15.0	-45.9	1.15E-07	1.9E-08	1.4E-09	7.4
140	-14.9		1.65E-07	1.1E-08		
140	-15.0	-47.1	1.69E-07	2.0E-08	1.1E-09	5.5
140	-15.0		1.70E-07	1.1E-08		
150	-14.3	-39.9	2.42E-07	5.5E-09	3.0E-10	5.5
150	-14.8	-40.6	3.40E-07	2.1E-08	1.2E-09	5.7
Average Value	-15.5	-44.7	1.97E-07	1.8E-08	1.2E-09	6.2

Figure B-7.

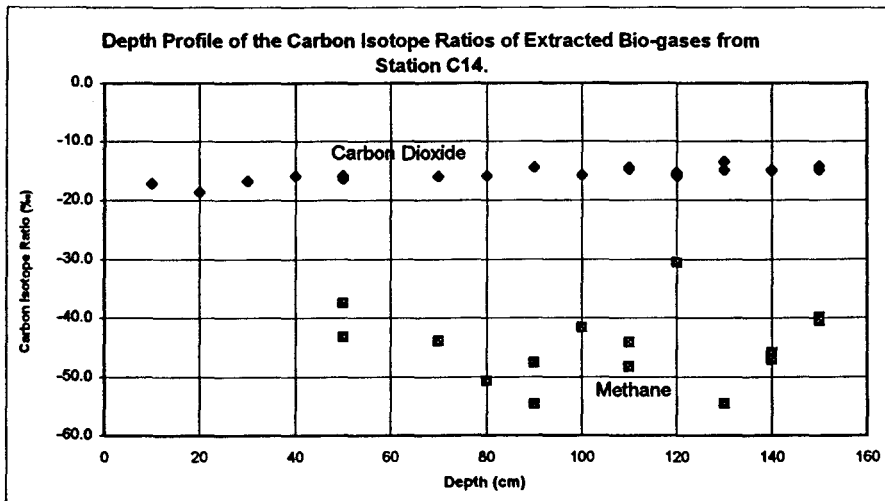


Table B-8. Isotopic Results from Station C15.

Station C15						
Depth (cm)	$\delta^{13}\text{C} - \text{CO}_2$ (‰)	$\delta^{13}\text{C} - \text{CH}_4$ (‰)	System Stability (Ratio 2/1)	Peak Area CO_2	Peak Area CH_4	Peak Area Ratio $(\text{CH}_4/\text{CO}_2)*100$
10						
20	-21.9		2.95E-07	4.6E-09		
30	-19.8		2.64E-07	4.4E-09		
40	-22.0		2.07E-07	6.1E-09		
50	-19.1		4.52E-07	2.5E-09		
60	-19.3		4.98E-07	3.6E-09		
Average Value	-20.4		3.43E-07	4.2E-09		

Figure B-8.

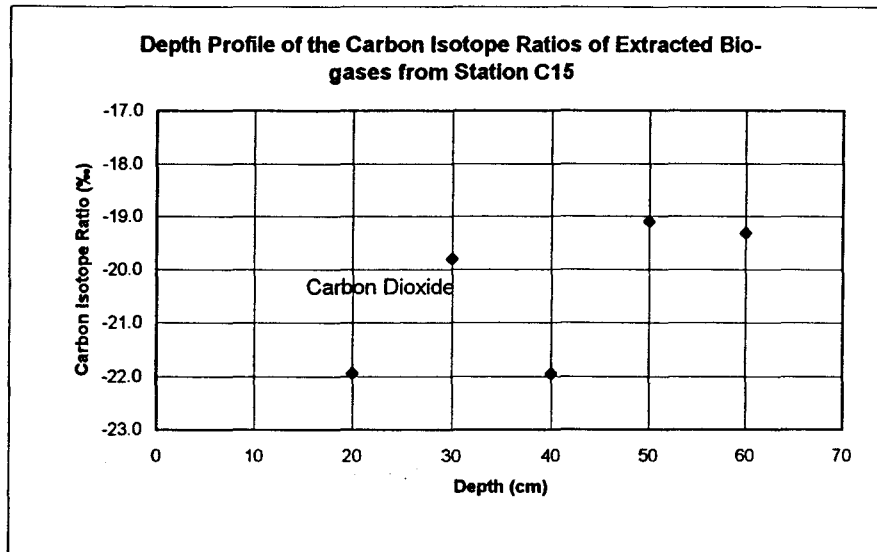


Table B-9. Isotopic Results from Station M7.

Station M7						
Depth (cm)	$\delta^{13}\text{C} - \text{CO}_2$ (‰)	$\delta^{13}\text{C} - \text{CH}_4$ (‰)	System Stability (Ratio 2/1)	Peak Area CO_2	Peak Area CH_4	Peak Area Ratio $(\text{CH}_4/\text{CO}_2)*100$
10	-22.8		1.63E-07	4.4E-09		
10	-23.1		1.11E-07	4.5E-09		
20	-21.3		1.01E-07	7.0E-09		
20	-21.6		3.67E-07	4.9E-09		
30	-19.1		1.99E-07	5.6E-09		
30	-19.1		1.27E-07	7.3E-09		
40	-16.9		2.42E-07	7.1E-09		
40	-17.0		1.47E-07	8.9E-09		
50	-15.2		3.90E-07	3.6E-09		
60	-14.4		3.92E-08	1.5E-08		
60	-14.4		4.73E-07	1.4E-08		
70	-14.1		2.34E-07	9.0E-09		
Average Value	-18.2		2.16E-07	7.6E-09		

Figure B-9.

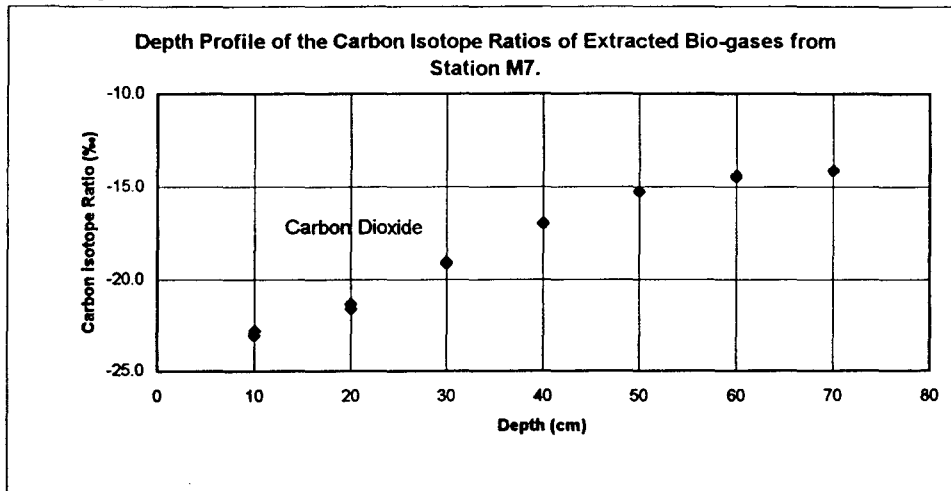


Table B-10. Isotopic Results from Station M11.

Station M11						
Depth (cm)	$\delta^{13}\text{C} - \text{CO}_2$ (‰)	$\delta^{13}\text{C} - \text{CH}_4$ (‰)	System Stability (Ratio 2/1)	Peak Area CO_2	Peak Area CH_4	Peak Area Ratio $(\text{CH}_4/\text{CO}_2)*100$
10	-17.4		1.68E-07	1.4E-08		
20	-17.0		4.27E-07	1.6E-08		
30	-14.8		2.75E-07	1.4E-08		
40	-17.4		1.53E-07	1.9E-08		
50	-15.5		2.99E-07	1.3E-08		
60	-16.3		2.67E-07	1.3E-08		
60	-16.6		3.63E-07	2.0E-08		
70						
80	-16.0		2.75E-07	1.8E-08		
90	-16.8	-47.2	3.93E-07	2.3E-09	4.4E-10	19.1
100	-17.4	-50.5	4.41E-07	1.7E-08	6.0E-09	35.3
110	-14.8	-54.7	1.66E-07	1.1E-08	2.6E-09	23.6
120	-14.6	-55.9	7.95E-08	1.4E-08	3.5E-09	25.0
130	-15.4	-47.3	1.16E-07	1.1E-08	5.1E-09	46.4
140	-18.1	-45.8	4.08E-08	7.4E-10	4.0E-10	54.1
Average Value	-16.3	-50.2	2.47E-07	1.3E-08	3.0E-09	33.9

Figure B-10.

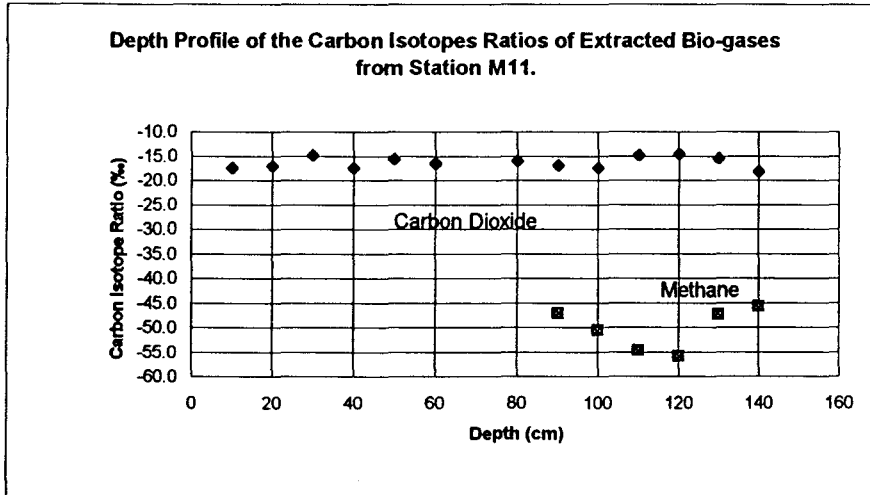


Table B-11. Isotopic Results from Station 0-8.

Station 0-8						
Depth (cm)	$\delta^{13}\text{C} - \text{CO}_2$ (‰)	$\delta^{13}\text{C} - \text{CH}_4$ (‰)	System Stability (Ratio 2/1)	Peak Area CO_2	Peak Area CH_4	Peak Area Ratio $(\text{CH}_4/\text{CO}_2)*100$
10	-19.2		1.19E-07			
20	-20.1		2.73E-07			
30	-18.7		1.10E-07			
30	-19.1		1.54E-08			
40	-15.5	-21.1	3.63E-07	5.2E-09	5.7E-09	109.6
40	-15.2	-23.3	1.47E-07	3.3E-09	2.5E-09	75.8
50	-15.2	-27.0	3.41E-07	2.3E-09	3.2E-09	139.1
60	-12.0	-27.1	1.92E-07	2.3E-09	2.6E-09	113.0
60	-11.5	-25.7	2.55E-07	2.7E-09	3.1E-09	114.8
70	-12.4	-26.7	2.33E-07	2.1E-09	2.1E-09	100.0
80	-14.3	-31.4	1.99E-07	1.6E-09	2.2E-09	137.5
Average Value	-15.7	-26.0	2.04E-07	2.8E-09	3.1E-09	112.8

Figure B-11.

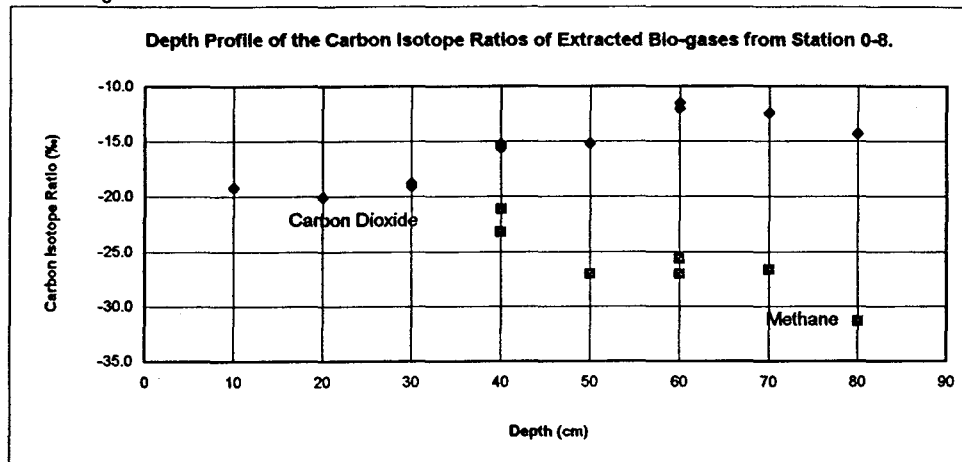


Table B-12. Isotopic Results from Station P4.

Station P4						
Depth (cm)	$\delta^{13}\text{C} - \text{CO}_2$ (‰)	$\delta^{13}\text{C} - \text{CH}_4$ (‰)	System Stability (Ratio 2/1)	Peak Area CO_2	Peak Area CH_4	Peak Area Ratio $(\text{CH}_4/\text{CO}_2)^*100$
10	-20.6		2.22E-07	1.6E-08		
20	-20.5		4.17E-07	1.7E-08		
30	-19.0		1.36E-07	1.6E-08		
40	-19.1		1.24E-07	1.4E-08		
50	-20.3		1.26E-07	1.8E-08		
60	-19.2		1.37E-07	1.3E-08		
70	-18.3		3.17E-07	1.3E-08		
80	-19.5		5.14E-08	1.9E-08		
90	-18.4		5.55E-07	1.5E-08		
100	-18.5		2.73E-07	1.4E-08		
100	-18.4		2.01E-07	1.7E-08		
100	-18.7		2.73E-07	1.2E-08		
110	-17.5		2.45E-07	1.7E-08		
120	-18.9		1.17E-08	2.0E-08		
130	-18.6		4.02E-07	4.4E-09		
130	-18.0		1.38E-07	1.4E-09		
130	-18.6		4.05E-08	1.7E-08		
140	-18.2		7.64E-08	1.2E-08		
140	-18.0		3.54E-07	1.3E-08		
140	-18.4		3.55E-07	1.1E-08		
150	-16.5		1.95E-07	1.2E-08		
Average Value	-18.7		2.21E-07	1.4E-08		

Figure B-12.

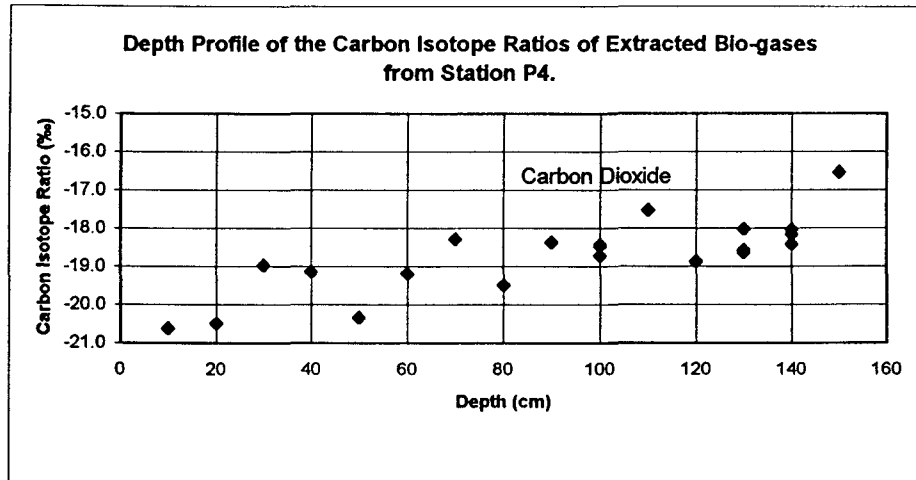


Table B-13. Isotopic Results from Station 2E8.

Station 2E8						
Depth (cm)	$\delta^{13}\text{C} - \text{CO}_2$ (%)	$\delta^{13}\text{C} - \text{CH}_4$ (%)	System Stability (Ratio 2/1)	Peak Area CO_2	Peak Area CH_4	Peak Area Ratio $(\text{CH}_4/\text{CO}_2)*100$
10	-19.4		1.55E-07	1.0E-08		
20	-19.7		2.95E-07	1.0E-08		
20	-19.9		7.77E-08	1.2E-08		
30	-18.8		1.04E-07	1.1E-08		
40	-19.1		1.51E-07	1.0E-08		
50	-18.3		2.41E-07	8.1E-09		
60	-16.1		2.40E-07	1.2E-08		
60	-16.1		4.65E-07	2.8E-09		
70	-14.9		3.59E-07	8.8E-09		
70	-14.6		1.34E-07	2.4E-09		
80	-14.4		8.13E-08	1.1E-08		
90	-14.5		1.39E-07	6.9E-09		
100	-13.5		1.64E-07	8.0E-09		
110	-13.4		1.48E-07	8.7E-09		
120	-13.5		1.56E-07	5.4E-09		
130	-15.0		2.08E-07	8.8E-09		
130	-15.1		1.91E-07	5.4E-09		
130	-14.8		1.13E-07	1.2E-08		
140	-15.1		1.45E-07	6.4E-09		
140	-14.9		2.89E-07	1.5E-09		
150	-13.0		1.35E-07	7.1E-09		
160	-13.2		1.34E-07	6.1E-09		
Average Value	-15.8		1.88E-07	7.9E-09		

Figure B-13.

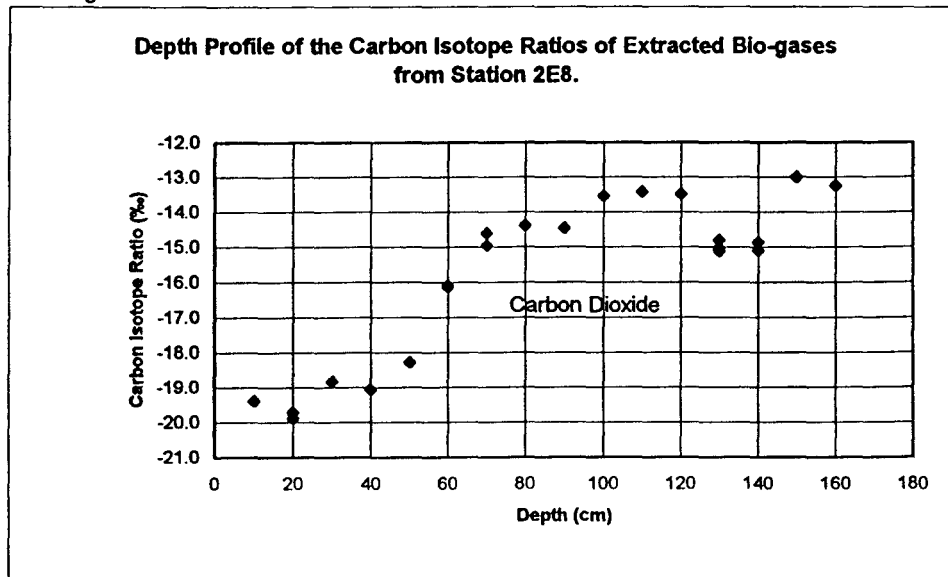
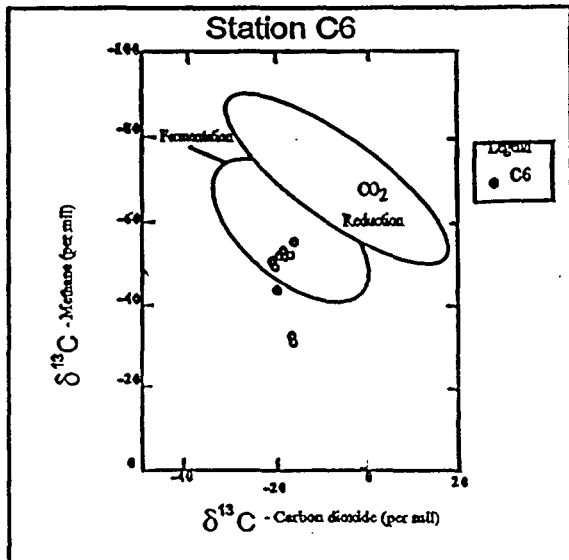
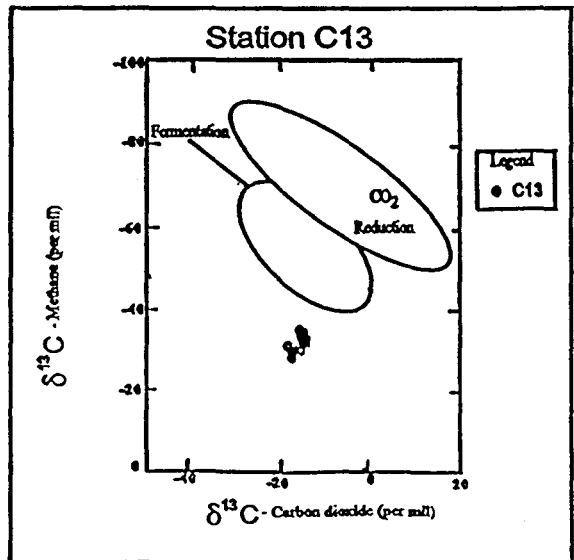
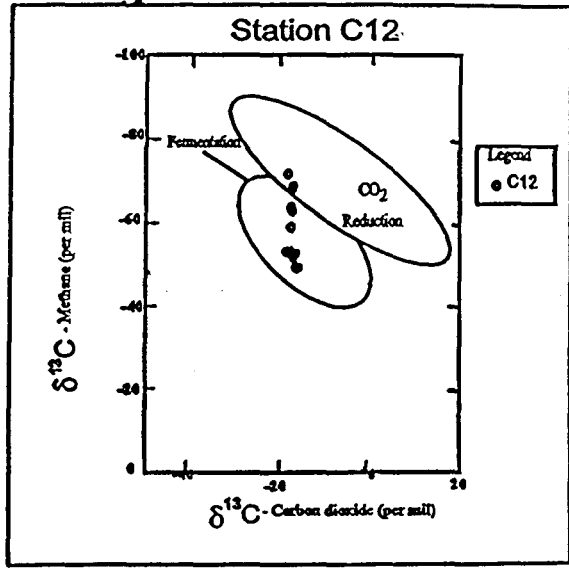
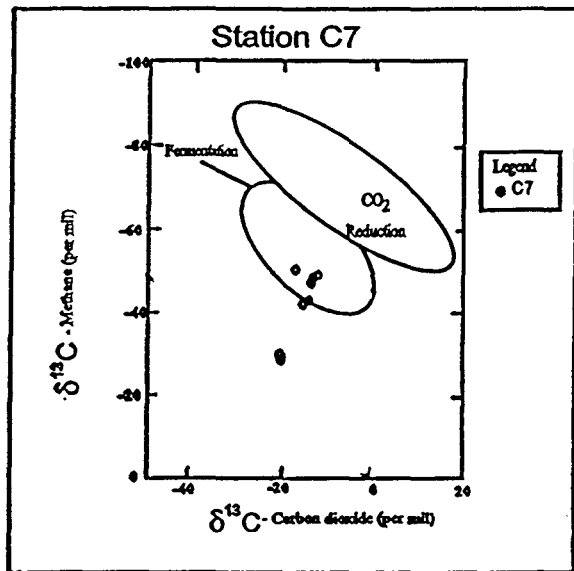
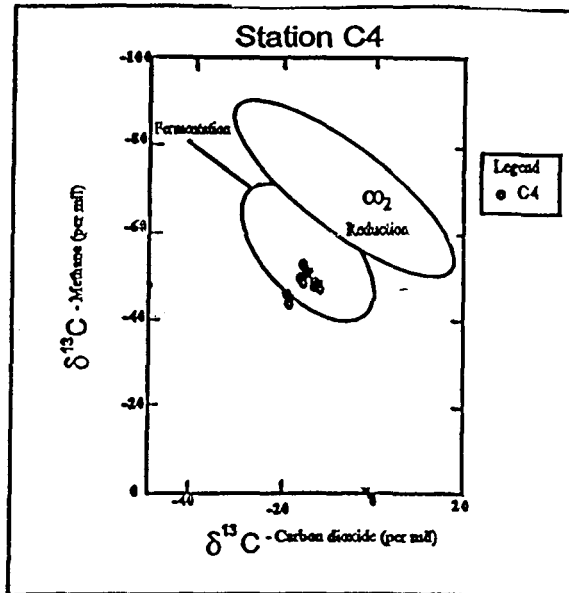
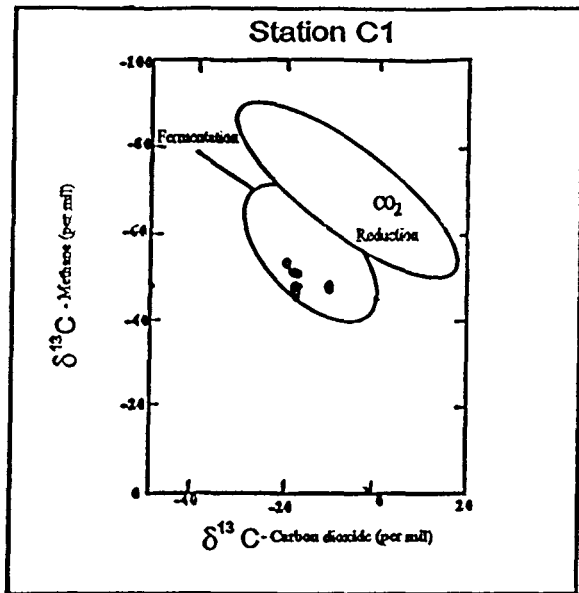


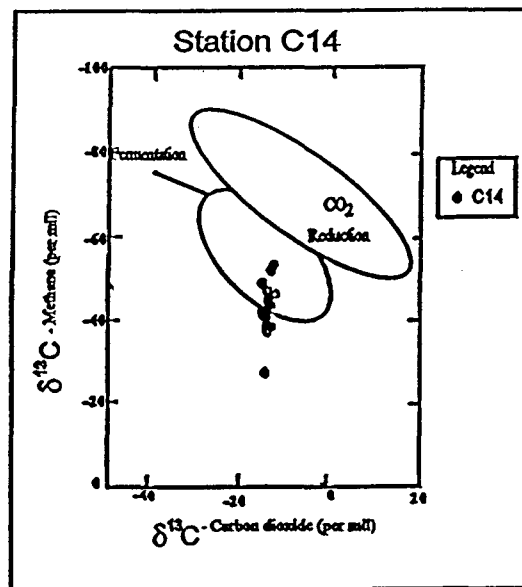
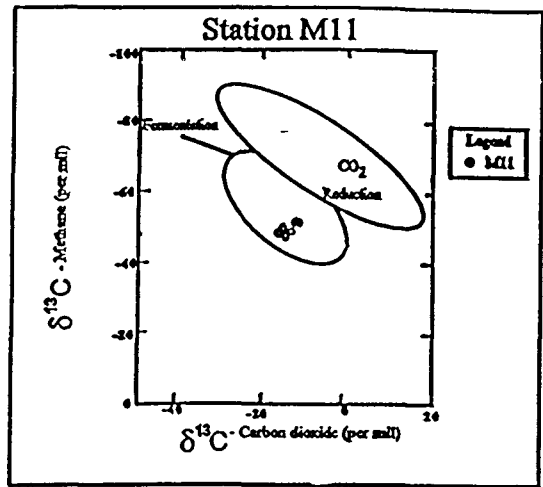
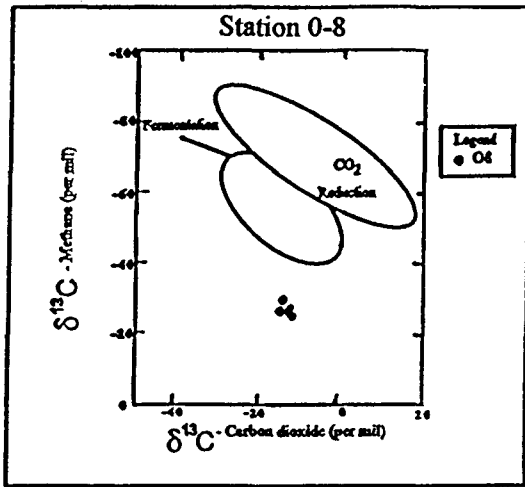
Table B-14. Isotopic Results from Other Stations.

All Other Stations							
Station	Depth (cm)	$\delta^{13}\text{C} - \text{CO}_2$ (‰)	$\delta^{13}\text{C} - \text{CH}_4$ (‰)	System Stability (Ratio 2/1)	Peak Area CO_2	Peak Area CH_4	Peak Area Ratio (CH_4/CO_2)*100
C2	50	-35.1	-58.4	1.49E-07	2.4E-09	1.5E-08	625.0
C3	50	-26.8	-61.3	2.75E-07	4.9E-09	4.6E-09	93.9
C5	50	-34.9	-44.7	3.08E-07	2.2E-09	6.3E-09	286.4
CO	50	-43.5	-68.9	1.42E-07	2.3E-09	1.2E-08	521.7
P5	50	-18.4		2.12E-07	2.8E-09		

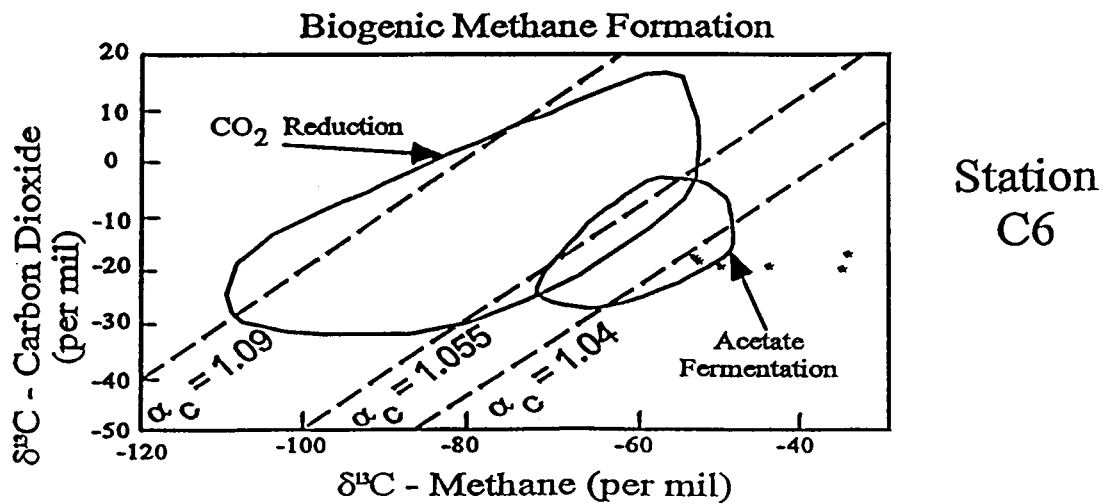
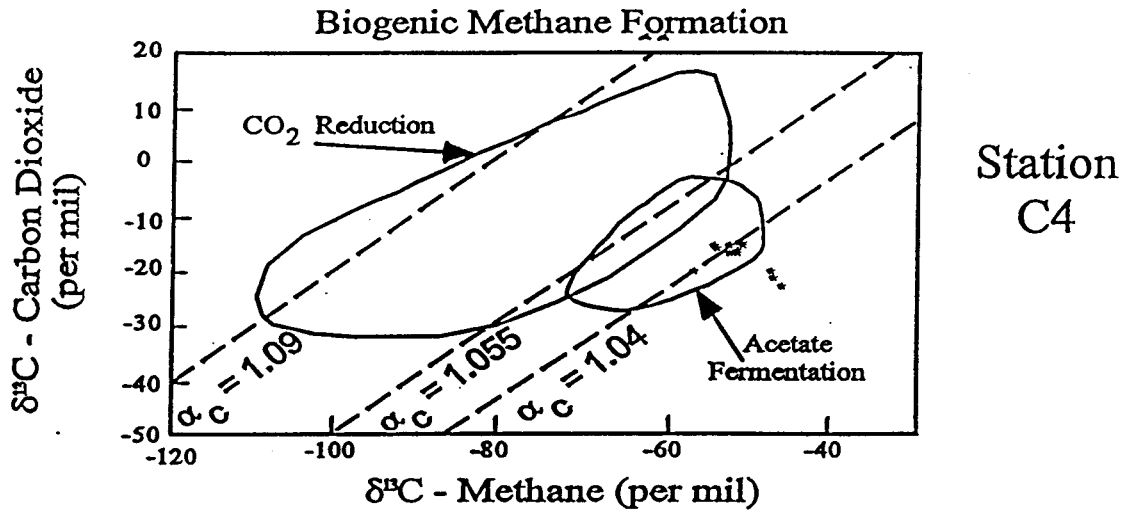
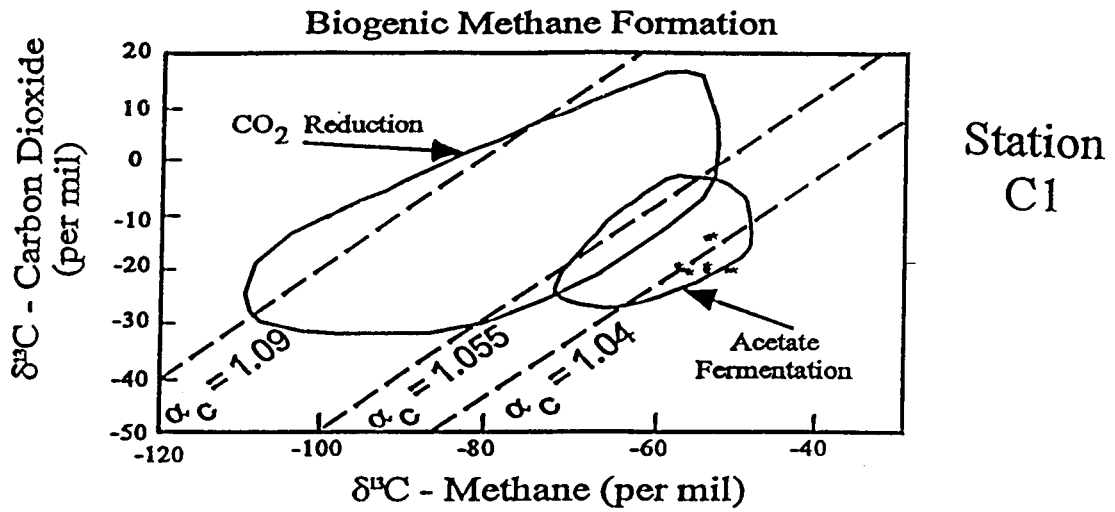
Figures B-14 to B-19. Cross-plot of the Carbon Isotope Ratios of Methane and Carbon Dioxide of Stations C1, C4, C7, C12, C13 & C6.



Figures B-20 to B-22. Cross plot of the carbon isotope ratios of methane and carbon dioxide of Stations 0-8, M11 and C14.



Figures B-23 to B-25. Cross plot of the carbon isotope ratios of methane and carbon dioxide of Stations C1, C4 and C6.



Figures B-26 to B-28. Cross plot of the carbon isotope ratios of methane and carbon dioxide of Stations C7, C12 and C13.

